DEPARTMENT OF TRANSPORTATION

Storm-Induced Slope Failure Susceptibility Mapping

Omid Mohseni, Principal Investigator
Barr Engineering Co.

January 2018

Research Project
Final Report 2018-05

LRRB
LOCAL ROAD RESEARCH BOARD

To request this document in an alternative format, such as braille or large print, call 651-366-4718 or 1-800-657-3774 (Greater Minnesota) or email your request to ADArequest.dot@state.mn.us. Please request at least one week in advance.

Technical Report Documentation Page

1. Report No. MN/RC 2018-05	2.	3. Recipients Accession No.
4. Title and Subtitle Storm-Induced Slope Failure Susceptibility Mapping		5. Report Date January 2018 6.
7. Author(s) Omid Mohseni, Cory Anderson, Mike Strong, Ryan Conway, Charles Hathaway, Aaron Grosser and Aaron Mielke		8. Performing Organization Report No.
9. Performing Organization Name and Address Barr Engineering Co. 4300 MarketPointe Dr., Suite 200 Minneapolis, MN 55435		10. Project/Task/Work Unit No. 11. Contract (C) or Grant (G) No. (c) 1002142
12. Sponsoring Organization Name and Address Minnesota Local Road Research Board Minnesota Department of Transportation Research Services & Library 395 John Ireland Boulevard, MS 330 St. Paul, Minnesota 55155-1899		13. Type of Report and Period Covered 14. Sponsoring Agency Code
15. Supplementary Notes http:// mndot.gov/research/reports/2018/201805.pdf		

16. Abstract (Limit: 250 words)

A pilot study was conducted to characterize and map the areas susceptible to slope failure using state-wide available data. The objective was to determine whether it would be possible to provide slope-failure susceptibility mapping that could be used by local road and highway officials to understand better where slope failure may occur. This would allow the possibility of taking preventative measures where indicated, or developing contingency plans for areas of likely failure. As a first step, a review of pertinent slope-failure literature was conducted to determine which past studies could offer information or guidance useful for developing the mapping. The review helped identify which methods and factors could be most effectively used in assessing susceptibility to slope failure. Then, using physics-based concepts, and making use of publicly-available topographic, soils, and hydrologic information, an approach was developed for using the data to identify conditions under which slope failure would be likely. This approach was incorporated into a GIS-based model that produced mapping wherein slopes were identified and assigned one of five levels (very high to very low) of slope-failure susceptibility. The model was tested against a relatively small area in Carlton County to confirm that the indicated susceptibility to failure correlated well with locations in which there was observable or documented slope failure. The method was then validated by applying it to small areas in Sibley and Carver Counties where slope failures had occurred. Having validated the underlying physics-based approach, the mapping was then expanded to two Carlton and Sibley Counties.

17. Document Analysis/Descriptors Slope failure, Coefficient of internal friction, Cohesion, Seepage, Geographic information systems, Slope stability, Storms		18. Availability Statement No restrictions. Document available from: National Technical Information Services, Alexandria, Virginia 22312	
19. Security Class (this report) Unclassified	20. Security Class (this page) Unclassified	21. No. of Pages 80	22. Price

Storm-Induced Slope Failure Susceptibility Mapping

FINAL REPORT

Prepared by:

Omid Mohseni
Cory Anderson
Mike Strong
Ryan Conway
Charles Hathaway
Aaron Grosser
Aaron Mielke
Barr Engineering Co.

January 2018

Published by:

Minnesota Department of Transportation
Research Services & Library
395 John Ireland Boulevard, MS 330
St. Paul, Minnesota 55155-1899

ACKNOWLEDGMENT

We are very grateful to Minnesota's Local Road Research Board (LRRB) for providing the funding that allowed us to collaborate with state and local highway professionals in working on this slope-failure susceptibility mapping project. We would especially like to acknowledge the members of the Technical Advisory Panel (TAP), who provided support, encouragement, and helpful guidance along the way. The TAP for this project included:

Farideh Amiri, MnDOT Research Services, (project coordinator)

Dan Sullivan, MnDOT Research Services, (project coordinator)

Paul Stine, MnDOT Operations Engineer, (technical liaison)

Jake Balk, Scott County Highway Department (construction manager)

Tim Becker, Sibley County Public Works (director)

Blake Nelson, MnDOT geotechnical engineer, Office of Materials and Road Research

Philip Schaffner, MnDOT director of Policy Planning

Mike Tardy, Carlton County Highway engineer

Joe Ulring, MnDOT State Aid Pavement engineer

TABLE OF CONTENTS

LIST OF FIGURES

LIST OF TABLES

ACRONYMS

DEM	Digital Elevation Model
GIS	Geographical Information System
ID	Intensity Duration
LiDAR	Light Detection and Ranging
LMIC	Land Management Information Center
LRRB	Local Road Research Board
MnDNR	Minnesota Department of Natural Resources
MnDOT	Minnesota Department of Transportation
MPCA	Minnesota Pollution Control Agency
NOAA	National Oceanic and Atmospheric Administration
NRCS	Natural Resources Conservation Service
NWS	National Weather Service
PFDS	Precipitation Frequency Data Server
SSURGO	Soils Survey Geographic Database
USCS	Unified Soil Classification System
USDA	United States Department of Agriculture

EXECUTIVE SUMMARY

With funding provided by Minnesota's Local Road Research Board (LRRB), Barr Engineering Co. (Barr) conducted a pilot project to characterize and map the areas susceptible to slope failure using statewide available data. The intent of the work was to determine whether it would be possible to provide slope-failure susceptibility mapping that could be used by local road and highway officials to understand better where slope failure may occur. This would allow the possibility of taking preventative measures where indicated, or developing contingency plans for areas of likely failure.

As a first step, Barr conducted a review of pertinent slope-failure literature to determine which past studies could offer information or guidance useful for developing the mapping. The review helped identify which methods and factors could be most effectively used in assessing susceptibility to slope failure.

Then, using physics-based concepts, and making use of publicly available topographic, soils, and hydrologic information, an approach was developed for using the data to identify conditions under which slope failure would be likely. This approach was incorporated into a GIS-based model that produced mapping wherein slopes were identified and assigned one of five levels (very high to very low) of slope-failure susceptibility.

The model was tested against a relatively small area in Carlton County to confirm that the indicated susceptibility to failure correlated well with locations in which there was observable or documented slope failure. The method was then validated by applying it to small areas in Sibley and Carver counties where slope failures had occurred. Having validated the underlying physics-based approach, the mapping was then expanded to two full Minnesota counties (Carlton and Sibley).

This report explains the methodology, discusses the data used, and presents the mapping results.

CHAPTER 1: INTRODUCTION

1.1 GENERAL DESCRIPTION AND GOALS OF THE PROJECT

Barr Engineering Co. (Barr) entered into a contract with the Minnesota Department of Transportation (MnDOT) in May of 2016 to complete a slope-failure susceptibility pilot project. Work was to be done through funding provided by the Local Road Research Board (LRRB) and done under the guidance and direction of a Technical Advisory Panel (TAP) consisting of experts from MnDOT and county highway departments. The objective of the work was to develop a GIS-based slope-failure susceptibility model that could be used to identify areas of susceptibility to slope failure in a given region.

The intent was to make use of existing research and geotechnical theory, along with statewide publicly available spatial data, to construct a slope-failure model that would have broad applicability. Another goal was to provide an indication of susceptibility at each location where there appeared to be a susceptibility to slope failure. Data from historical or existing slope failures would be used to calibrate/validate the model. The central product of the work would be maps showing areas where slope failure is likely and the expected susceptibility level.

Slope-failure risk mapping was to be produced for two (dissimilar) Minnesota counties as part of this pilot project. If the model development and mapping project was seen as successful, the thought was that subsequent work might allow for the expansion of the mapping to other Minnesota counties.

The work has the potential to improve road safety. It might allow preventive measures to be taken in areas where slope failure can be expected, thus avoiding costly repairs and economic damages to local communities.

1.2 WORK INVOLVED

Several steps were required for the development of the slope-failure susceptibility model and mapping. Greater detail is provided in the report sections that follow, but the steps included:

- **Conducting a literature review**—As a preliminary step in the process, a literature review was conducted to provide a general cataloging of research on slope failure causes, predictive methods, and mapping. Particular attention was paid to research that sought to identify failure mechanisms and algorithms and research that sought to result in slope-failure susceptibility mapping. Key failure-risk factors were identified. Results of the literature review conducted for this project have been presented separately to the Technical Advisory Panel (TAP).

- **Collecting and reviewing data from known slope-failure sites**—Barr collected site-specific slope-failure data from various sources. The intention was to use the data to identify any important failure-risk factors that might not have been identified through the literature review. The data was also to be used for subsequent testing of the slope-failure model. These included

Barr's own project data (including that from substantial work on slope repair along Highway 210 in Carlton County) as well as other state and county sources.

- **Assembling and reviewing relevant geo-referenced datasets**—One of the goals of the slope-failure model development was to ensure that it was relatively simple and could be implemented using only generally available data. Therefore, it was necessary to review the statewide datasets that were available and examine them to ensure that they would, in fact, provide information that was both relevant and useable. We looked at and considered several such data but eventually determined that only a few would be applicable for use with our GIS-based model.

- **Developing GIS-based slope-failure model**—At the center of the work was the development of a slope-failure model. The model needed to use the previously identified key failure-risk factors as part of a predictive equation that could be used with spatial data and used broadly to provide the GIS susceptibility mapping. It made use of generally accepted geotechnical slope-failure theory, generally-available soils characteristics data, and probability factors inherent in the Atlas 14 hydrologic data. Coding was then necessary to incorporate the model into the GIS mapping software.

- **Testing the model using data from known sites of slope failure**—With the model developed and the algorithm incorporated into the GIS software, the results were tested against areas of known slope failure. This allowed further refinement of the model and better identification of the soil parameters that could be used most effectively.

- **Developing final statewide slope-failure risk maps**—After the model was refined and we were confident that the results it was producing would have broad applicability, we expanded the mapping to two entire counties – Sibley and Carlton. Mapping results are provided and discussed in subsequent sections of this report.

- **Coordination with the TAP**—Throughout the project, we coordinated with the TAP to ensure that the project was proceeding in the right direction. Kickoff and progress meetings were held, we presented and sought comments on the literature review, and preliminary modeling results were demonstrated to allow the TAP to provide feedback and suggestions on how the results might be best presented. The final report was also reviewed by the TAP and adjusted where necessary based on the reviewers' comments.

1.3 TIMELINE

The contract for this project was signed in May of 2016, with 1 year allowed for the project's completion. The work was completed in February of 2017, approximately 3 months ahead of schedule.

1.4 STRUCTURE OF THIS REPORT

The remainder of this report describes the process by which we reviewed the relevant research, identified and assembled the available and useful datasets, developed a slope-failure susceptibility model, tested results against areas of known slope failure, and categorized and mapped slope-failure susceptibility for two counties.

Subsequent sections of this report therefore provide discussions of the following:

- Literature review findings
- Available statewide datasets used in the analysis and mapping
- Model development
- Programming and GIS analysis
- Model calibration and validation of the results
- A summary of review of the geotechnical assumptions and revising of the hydrological analysis
- Results and potential applications of the mapping

A final section provides an overall project summary, and general conclusions. In addition, three appendices are provided to describe in detail the literature review (Appendix A), review of the geotechnical assumptions (Appendix B), and a revision of the hydrologic analysis (Appendix C). Appendices B and C were completed as an extension to the original contract.

CHAPTER 2: LITERATURE REVIEW FINDINGS

2.1 APPROACH

The purpose of the literature review conducted for this study1 was to survey the range of available information regarding landslide susceptibility. For the review, previous studies were identified, summarized, and cataloged. We also identified information and causative factors that appear to be relevant to landslides in Minnesota.

Given the limited scope of the present project for the LRRB, a comprehensive review of all available literature could not be undertaken. Therefore, we focused on studies that appeared to have application to Minnesota (i.e., studies done in areas with similar geography, landscapes and climate), and that were conducted by government agencies such as state transportation departments and the US Geologic Survey. We attempted to identify and examine the most-referenced papers in this field, as well as papers that described studies with aims similar to those of this project.

2.2 SUMMARY OF AVAILABLE RESEARCH

Our review of the literature revealed that the creation of landslide, debris flow and/or slope failure occurrence inventories is common practice in many regions of the world. In addition, many studies have been conducted that attempt to quantify the likelihood of the occurrence of landslides or identify areas that have the propensity to produce these phenomena.

However, landscape processes and triggers tend to be unique to a specific geography. As a result, only a small number of reviewed studies seem to have applicability for Minnesota. Despite this limitation, the published studies provide valuable information on methods of analysis that may be used for this project.

2.2.1 Inventories

The first step in most landslide and slope-failure susceptibility studies is compiling an inventory of historical slope failures. Landslide processes have been found to have a legacy effect—landslides follow landslides. Therefore, inventories of past failures can be used to determine where future failures are likely, based on spatial and temporal information.

The utility of landslide inventories is limited because that they tend to over-report landslides in developed areas, and tend to focus on recent landslides. Although a given geographic area may not have

---

1 The complete literature review is provided as Appendix A to this report. It includes a listing and brief summary of the reviewed papers and reports.

documented historic landslides, it may still be susceptible to landslides. Attempts are being made to increase the size of historical landslide databases by utilizing LiDAR data to identify failures based on ground surface morphology.

In Minnesota, the Department of Natural Resources (MnDNR) has recently completed a study to inventory historical failures in the Twin Cities Metropolitan area using a variety of archival records. These records span the period from 1979 to 2014. Reportedly, the MnDNR intends to complete a more comprehensive, statewide inventory at some point in the future.

2.2.2 Susceptibility Analyses

Many landslide susceptibility studies have been published, and both qualitative and quantitative approaches have been applied. The most common approaches can be grouped into four categories: (1) geomorphic hazard mapping; (2) index-based methods; (3) statistically based methods; and (4) physically-based methods.

- Geomorphic hazard mapping of landslide susceptibility is a qualitative method that uses subjective expert judgement to identify actual and potential slope failures.
- In index-based methods, spatial distribution of causative factors are identified and their influence on observed failures are weighted.
- In statistical methods, multivariate statistical techniques are used to develop function relationships between causative factors and observed failures.
- Physically-based methods apply process-based geotechnical models, like the infinite slope stability model, to evaluate failure conditions from a set physical parameters.

2.3 MAJOR CAUSATIVE FACTORS

The review of literature conducted for this study suggested that there is a finite list of major causative factors of landslides and slope failure relevant for Minnesota. These factors are summarized below. Because the factors influencing slope failure are unique to a particular location and set of circumstances, it cannot be said that any of the factors is universally more important than the others.

SLOPE ANGLE

Other factors being equal, steeper slopes are more prone to landslides and slope failure than shallower slopes. A number of studies have identified slope angle ranges where landslides are most likely to occur for a given geography. However, other studies have shown that slope angle alone is not sufficient to gauge how vulnerable an area is to landslides. Other factors can cause a relatively steep slope to be stable, while a relatively shallow slope may be landslide prone.

SOIL TYPE AND GEOLOGY

The geotechnical properties of a soil (shear strength, permeability etc.), are significant factors in determining landslide susceptibility. Soils with a high shear strength are less susceptible to landslides than soils with a lower shear strength. The hydraulic soil properties of the soil are also important because these properties affect what intensity and duration of rainfall event is required to initiate a landslide.

VEGETATION

At least one of the papers reviewed observed a correlation between vegetation and landslides, with the majority (56%) of landslides in the study area (Maryland) occurring in areas with low- to medium-density grass. As discussed by Duncan and Wright (2005), woody vegetation (trees and large shrubs), provide mechanical reinforcement to the soil, as well as reducing infiltration and providing erosion protection and generally helping to protect against shallow sliding.

LAND USE AND DRAINAGE DENSITY

Characteristics of the drainage area at and above a slope—including drainage density and land use changes—are related to the geomorphology of a landscape. Drainage density calculations provide an estimate of the area prone to soil saturation, which is a major factor of slope failure.

ANTECEDENT PRECIPITATION/SOIL MOISTURE

In many climatic regions, antecedent precipitation has been found to be related to occurrence of slope failures. Cumulative rainfall threshold relationships have been developed for specific geographies. These relationships are defined by parameters such as the total rainfall amount during the past 3 days, and the total rainfall amount during the previous 15 days (Seattle, Washington area); or the 1-, 2-, 7-, 30-, and 90-day antecedent precipitation (southwest United Kingdom).

Other studies have attempted to couple hydrologic models with simple slope-stability models to predict locations of shallow landslides. The hydrologic models are used to calculate soil saturation based on contributing drainage area, soil transmissivity, and local slope. Then the “infinite slope stability model” (often used in slope stability evaluations) is used, with degree of soil saturation as an input parameter.

RAINFALL INTENSITY AND DURATION

Many studies have found rainfall intensity and duration to be related to occurrence of slope failures. Empirical intensity-duration (ID) threshold relationships have been developed to try to identify conditions under which failures would be initiated. Many of these ID thresholds are unique to the climatic regions for which they were developed. However, global ID thresholds have been developed by

normalizing the precipitation data by the mean annual precipitation and the “rainy-day normal” (which is the ratio of the mean-annual-precipitation to the average number of rainy days in a year).

The literature review identified the six factors (above) that researchers have seen as having correlation with slope failure. However, our assessment was that only three of these factors (slope angle, soil type, and rainfall depth) had practical utility in developing the slope-failure model. Section 4.0 of this report describes how slope angle, soil type, and rainfall depth were used in model development. While land use and drainage density remain important factors in landslide occurrences, yet their inclusion posed complications for developing a workable model.

CHAPTER 3: AVAILABLE STATEWIDE DATA

3.1 LIDAR DATA

The model benefits from the availability of high-quality LiDAR data for the entire state of Minnesota. This data was collected under a number of different programs between 2008 and 2012. This LiDAR data is publicly available online through the Minnesota Department of Natural Resources (MnDNR) MnTopo web interface, or through an FTP site hosted by the state's Land Management Information Center (LMIC). The LiDAR data is relatively current; Carlton County, along with the Arrowhead counties, were surveyed in the spring of 2011 by Woolpert, Inc. under the supervision of the MnDNR. Sibley County was surveyed along with 25 other Minnesota River basin counties in 2010 by AeroMetric Inc. (now Quantum Spatial) with the work also performed under the supervision of the MnDNR.

The statewide LiDAR data is available preprocessed as a 1-meter or 3-meter resolution file geodatabase raster for use in Esri's ArcGIS software. The current project made use of the 3-meter resolution raster. Using the lower-resolution raster greatly reduces the time required to process large datasets, which is particularly important at a statewide scale. The 3-meter raster was also determined to better capture the representative slope of the ground surface because it smooths the pits and bumps of the 1-meter surface – those pits and bumps indicating slope discontinuities that are unimportant for purposes of this project.

The GIS-based model utilizes a 3-meter slope raster (in degrees) derived directly from the LiDAR dataset. This slope raster is processed using the standard "Slope" tool in the ArcGIS Spatial Analyst toolbox. Surface slope is an important factor in predicting slope failure. Because of this, it should be noted that it would be difficult to utilize this model in areas where high-resolution topographic data is unavailable.

3.2 SSURGO DATASET

The United States Department of Agriculture (USDA) Natural Resources Conservation Service (NRCS) has published and regularly updates the Soil Survey Geographic Database (SSURGO) for most of the United States. This database consists of seamless-coverage soil map units delineated by their unique attributes. The attributes can generally be broken into two categories: soil suitability or limitations for use, and soil physical properties and qualities. Identification of soil types is provided in the database in accordance with the Unified Soil Classification System (USCS).

The data can be accessed and downloaded via the USDA NRCS Web Soil Survey website by a custom Area of Interest (up to 100,000 acres) or by County. The data is seamless, but because it is created and maintained based on county boundaries, inconsistencies can be found in the data at county lines.

The SSURGO database provides soil information for the top 6 feet of the area in question. This gives it applicability for a predictive model for shallow slope failure.

Once acquired, the SSURGO data was processed using the NRCS-provided custom Soil Data Viewer toolbar for Esri ArcGIS. This toolbar allows convenient processing of the SSURGO database to view more than 100 different soil properties. The user can also set a specific soil depth range to query (up to approximately 6 feet). The data is not complete; some soil properties may not be available for a particular area or county. Agricultural areas appear to have a more complete record in the database than non-agricultural areas.

The SSURGO dataset is used for several model inputs. For each USCS soil type, the plasticity index, soil bulk density (in g/cm^3 at 1/3 bar), and soil texture (the soil's relative ratios of sand, silt and clay) are processed using the Soil Data Viewer toolbar. The results of the queries, at a map unit scale, are then used to determine other soil characteristics needed for the model. It is important to note that all data obtained from the SSURGO database provides only estimates of soil characteristics—both in their spatial extent and their specific values. Providing more accurate and spatially-precise values would require site-specific soil testing.

3.3 ATLAS 14 DATA

The National Oceanic Atmospheric Administration (NOAA) National Weather Service's (NWS) Atlas 14 data provides the amount of precipitation for storms of varying durations, along with the likelihood of their occurrence expressed as exceedance probabilities. The data is spatially related in that it provides an estimated precipitation amount (in inches) for a given storm in a given geographical location. This information is stored in raster format with a cell size of approximately 900 by 900 meters for the state of Minnesota. Rainfall amounts for a given storm can vary by several inches, depending on location and storm duration.

Atlas 14 data is publically available via the NWS Hydrometeorological Design Studies Center's Precipitation Frequency Data Server (PFDS).

CHAPTER 4: SLOPE-FAILURE MODEL DEVELOPMENT

4.1 SUMMARY OF PREVIOUS PHYSICS-BASED APPROACHES

A number of researchers in past decades have attempted to use geographic information system (GIS) and physics-based approaches to model and predict slope failure. One of the first studies was conducted by Montgomery and Dietrich (1994) using the infinite slope stability theory and the hydrologic model TOPOG. TOPOG used a steady state rainfall to map the spatial pattern of saturated surficial soils. The results of the approach was applied to three watersheds in California, Oregon, and Washington states to determine areas unconditionally stable and unstable, and areas with different ranges of rainfall intensity to become unstable, i.e. resulting in slope failure.

The Montgomery and Dietrich work was extensively referenced by other researchers who used a physics-based method for predicting slope failures. Casadel et al. (2002) used Montgomery and Dietrich's approach and expanded the model by calibrating four hydrologic parameters to characterize the saturated hydraulic conductivity of the soil and underlying bedrock to predict the timing and location of shallow landslides in hilly and mountainous areas.

Iida (2004) developed a model incorporating deterministic aspects of slope stability and stochastic character of rainfall intensity and duration. He used the infinite slope stability theory and predicted the probability of the critical saturated soil susceptible to failure. He used a digital elevation model (DEM) and predicted the average recurrence interval of storms for each grid cell that exceed the critical saturated condition in soil.

D'Odorico et al. (2005) developed a model to study the effects of unsteady rainfall infiltration in hillslopes. They used the infinite slope stability theory, and coupled it with simple hydrograph models and intensity-duration-frequency curves to determine the return period and the associated critical storm duration of landslide triggering rainfall events.

Rosso et al. (2006) developed a model by coupling infinite slope stability theory and hillslope hydrology and accounted for both storm duration and intensity in triggering shallow slope failures.

In all of these studies, the infinite slope stability theory was used as the basis of a deterministic approach to predict shallow slope failure. After reviewing the statewide data that was available, and considering other possible approaches (e.g., regression analysis), for our GIS-based model we decided to also use the fundamentals of the infinite slope stability theory to estimate susceptibility to failure in shallow slopes.

The following sections provide an explanation of the theory and its use for our model.

4.2 MATHEMATICAL MODEL

In slope failure events, the plane of failure is very complex but it is commonly simplified as an arc-shape, as shown on **Error! Reference source not found.** However, the simplest way of analyzing slope stability is to assume that the plane of failure is parallel to the slope with an unlimited extent as shown in Figure 4.2. This method of analysis of slope stability is known as the infinite-slope theory and was first introduced by Culmann in 1866. Résal modified it in 1910 by accounting for pore pressure (Winterkorn and Fang, 1975).

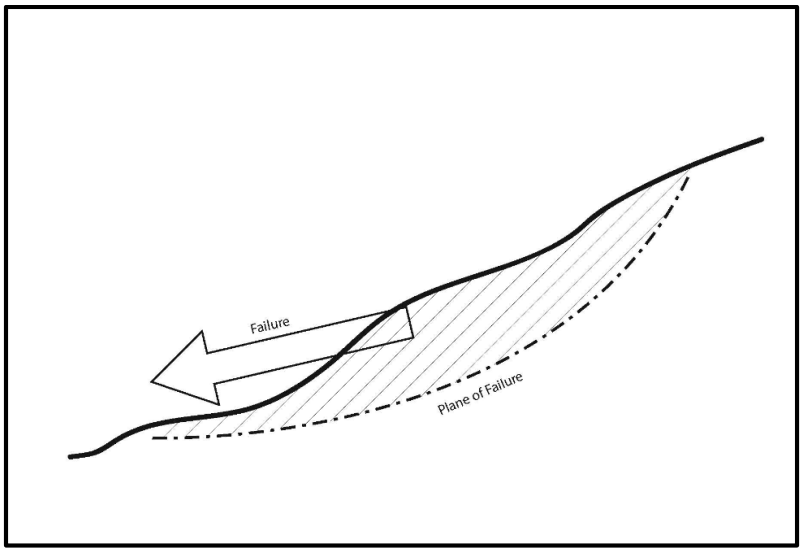

Figure 4.1 Arc-shaped plane of failure

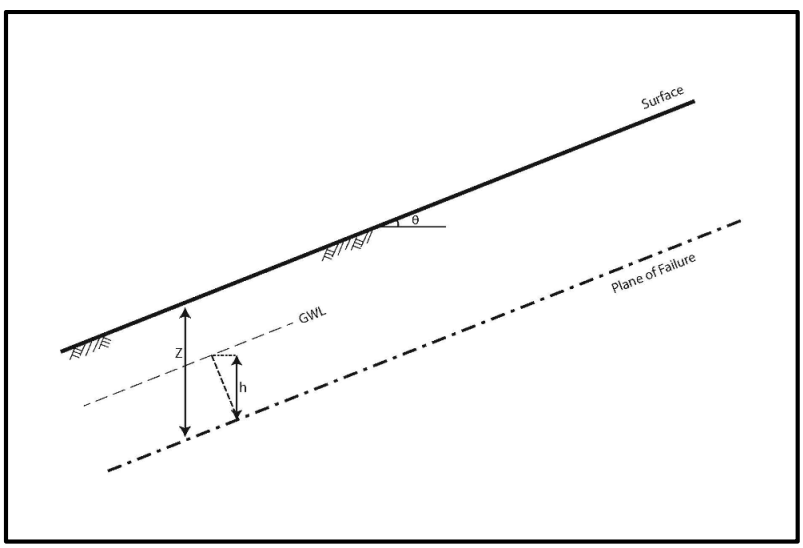

Figure 4.2 Schematic for infinite slope stability theory showing model parameters

Using the infinite slope stability theory, one can determine conditions under which a soil layer with a thickness of Z will slip over a plane parallel to the surface, which has a slope angle of θ with horizon. The slipping conditions can be determined using Coulomb's law of friction. Assuming seepage being parallel to the plane of failure, the factor of safety (FS) for slope failure along plane AB in **Error! Reference source not found.** can be determined from Equation 4.1 (Okimura, 1985).

$$\boldsymbol{FS} = \frac{\hat{C}+[(\gamma_{sat}-\gamma_w)\, h/\cos^2\theta + \gamma(Z-h/\cos^2\theta)]\cos^2\theta\,.\tan\hat{\varphi}}{[\gamma_{sat}h/\cos^2\theta + \gamma\,(Z-h/\cos^2\theta)]\sin\theta\,.\cos\theta} \qquad \textbf{Equation 4.1}$$

In Equation 4.1, $\hat{C}$ is the apparent cohesion, γ_{sat} is the specific weight of saturated soil, γ_w is the specific of water, $h/\cos^2\theta$ is the depth of seepage and h is the water pressure associated with the seepage depth (see Figure 4.2), γ is the unit weight of soil under normal conditions, θ is the slope angle, and $\hat{\varphi}$ is the effective internal angle of friction.

A factor of safety less than 1 results in slope failure. That is, if the numerator of Equation 4.1 is less than its denominator, the soil layer with a thickness of Z will slip over the plane of failure.

If Equation 4.1 is written as an inequality to indicate a condition wherein the factor of safety is smaller than 1, it can then be rearranged to define the minimum depth of seepage in the soil layer that is necessary to induce slope failure. In this way one can determine the minimum seepage depth (H_{cr}) required for causing slope failure:

$$\boldsymbol{H_{cr}} = \frac{\frac{\hat{C}}{\gamma_w} - SG.Z.\cos^2\theta(\tan\theta - \tan\hat{\varphi})}{\cos^2\theta\,[(SG_{sat}-SG)\,(\tan\theta - \tan\hat{\varphi}) + \tan\hat{\varphi}]} \qquad \textbf{Equation 4.2}$$

In Equation 4.2, H_{cr} is the critical seepage depth for the soil layer; SG is the bulk specific gravity of the soil, which is the ratio of the unit weight of soil to the unit weight of water; and SG_{sat} is the specific gravity of saturated soil. Note that the critical water pressure (h_{cr}) associated with the critical seepage depth is equal to $H_{cr}\cos^2\theta$.

4.3 APPROACH TO THE HYDROLOGIC ASPECTS OF THE MODEL

While Equation 4.2 is a relatively simple representation of slope stability, it incorporates all the necessary information to develop a GIS-based model to predict conditions under which a sloped area (or in a GIS context, an areal grid cell) would slip or would be susceptible to landslide or failure. Equation 4.2 can be used for the GIS-based model if one assumes that critical depth of water in soil is a direct reflection of rainfall events.

As indicated in Section 4.1, other researchers used hydrologic models to develop slope stability predictive tools. However, those approaches were never applied to a broad area such as a county or an entire state. A hydrologic model that would be coupled with the infinite slope stability theory would require parametrization of infiltration and groundwater flow, and would make the overall model impractical for the purpose of this broad-scale project. To avoid this problem, one can make the

simplifying assumption that all rainfall is infiltrated into the soil to the depth of plane of failure before any surface runoff occurs. Having made this assumption, Equation 4.2 can be used directly for calculating the amount of rainfall that will result in a critical seepage depth (h_{cr}) in the soil.

During the early development of the GIS-based model, attempts were made to determine and incorporate the drainage area of each grid cell of LiDAR data so as to better estimate the soil moisture situation at any given location. However, it was determined that without an accompanying detailed hydrologic model and a shallow groundwater model, attempting to use the drainage area of grid cells would create unmanageable difficulties and inconsistencies in the overall GIS-based slope-failure model. Therefore, it was assumed that each grid cell surface in the GIS-based model receives water from rainfall events, and that water infiltrates into the soil below. Surface runoff and water received from or flowing out to adjacent cells is not accounted for.

4.4 USE OF SSURGO DATASET IN THE MODEL

Equation 4.2 requires the slope angle θ, which can be generated from LiDAR data. The other parameters needed for use of the equation are soil parameters. These parameters must be either estimated or inferred from the SSURGO data. The methods for determining the needed parameters are explained in the remainder of Section 4.4.

The SSURGO dataset provides soil type information on soil characteristics for each USCS soil type. The internal friction angle φ can be determined by cross-referencing a table correlating the soil type to an approximate angle as shown in Table 4.1 (based on NRCS data). For clayey, cohesive soils (for example, soils listed as CH – Fat Clay, or CL – Lean Clay), the internal friction angle can be estimated using a plasticity index based on the relationship developed by Terzaghi et al. (1996). The limitation to this approach is that only the soil type in the surface layer is used; deeper soil layers are not considered. Nevertheless, preliminary review and model testing indicates that the surface-soil-type correlation is still a good way to approximate the internal friction angle.

The apparent cohesion parameter in Equation 4.2 can also be estimated from Table 4.1. It is important to note that *apparent* cohesion may be different from the values shown in Table 4.1. Variation would be expected due to consolidation, and the presence of root systems within the soils of vegetated slopes.

In the development of the GIS-based model it was initially assumed that cohesion would need to be a calibration parameter. However, as is shown in Section 6.0, the cohesion values shown in Table 4.1 provide reasonable estimates for use with the model.

Table 4.1 Relationship between Soil Type and Internal Angle of Friction

USCS Soil Class	Description	Friction angle, φ (°)	Cohesion, C (kPa)
GW	well-graded gravel, fine to coarse gravel	40	0
GP	poorly graded gravel	38	0
GM	silty gravel	36	0
GC	clayey gravel	34	0
GM-GL	silty gravel	35	0
GC-CL	clayey gravel with many fines	29	3
SW	well-graded sand, fine to coarse sand	38	0
SP	poorly graded sand	36	0
SM	silty sand	34	0
SC	clayey sand	32	0
SM-SL	silty sand with many fines	34	0
SC-CL	clayey sand with many fines	28	5
ML	silt	33	
CL	clay of low plasticity, lean clay	27	20
CH	clay of high plasticity, fat clay	22	25
OL	Organic silt, organic clay	25	10
OH	Organic clay, organic silt	22	10
MH	Silt of high plasticity, elastic silt	24	5

Soil composition is used to determine the soil's field capacity, whereas the bulk density is used to determine soil porosity. Together, field capacity and porosity can indicate the fully saturated weight of soil, at a given depth.

As stated in Section 3.0, the SSURGO dataset provides information on the bulk density of soil in grams per cubic centimeter (g/cm^3). Because water has a density of 1 g/cm^3, and bulk specific gravity is determined by dividing the bulk density by the specific gravity of water, the bulk specific gravity (SG) of the soil layer can be said to be equal to its bulk density.

The saturated specific gravity SG_{sat} can be estimated using the soil porosity and by assuming the initial moisture content of soil being at field capacity, ϑ_{FC}, which is the moisture content above which the soil layer is drained by gravity. Therefore SG_{sat} can be estimated from Equation 4.3:

$$\boldsymbol{SG_{sat} = SG + (\eta - \vartheta_{FC})} \qquad \textbf{Equation 4.3}$$

In Equation 4.3, η is porosity and ϑ_{FC} is moisture content of soil at field capacity. The field capacity of different soil types was approximated using Table 4.2.

The field capacity of different soil types was approximated using SSURGO information and field capacity data (MPCA, 2017) for specific soil types as shown in Table 4.2. The SSURGO dataset provides percent sand, silt and clay for each soil type in its database. Based on percent sand, soil and clay, the soil types were defined as shown in Table 4.2. Subsequently, the associated field capacities were determined from Table 4.2 and were incorporated in Equation 4.3.

Table 4.2 Field Capacity Data for Different Soil Types

Soil	Field capacity
Sand	0.17
Loamy sand	0.09
Sandy loam	0.14
Loam	0.25 - 0.32
Silt loam	0.28
Clay loam	0.32
Silty clay loam	0.30 -0.37
Clay	0.32

Assuming a grain-size specific gravity of 2.65 for non-organic soils, soil porosity was approximated from Equation 4.4:

$$\boldsymbol{\eta = 1 - \frac{SG}{2.65}} \qquad \textbf{Equation 4.4}$$

With an initial moisture content at field capacity, ϑ_{FC}, i.e. drained conditions for all soils, the minimum amount of infiltrating water (F) that will cause failure becomes:

$$\boldsymbol{F = h_{cr} \cos^2 \theta \, (\eta - \vartheta_{FC})} \qquad \textbf{Equation 4.5}$$

4.5 USE OF ATLAS 14 DATA IN THE MODEL

In the model, the parameter F (Equation 4.5) is the minimum amount of infiltrated rainfall which would cause slope failure. It was therefore necessary to estimate the amount of rainfall that would infiltrate during various storm events.

It is well known that during storm events, all rainfall does not infiltrate; some becomes surface runoff. In addition, there is a lateral movement of infiltrated water in hillside or alpine areas which can either increase or decrease the soil saturation in a particular section of a sloped area.

For the GIS-based model developed for this project, however, the simplifying assumption was made that there would be no surface runoff. Similarly, it was assumed that there would be no lateral transport of water within the soil layer from one grid cell to an adjacent one. It is understood that this approach is not hydrologically rigorous, yet it nevertheless allows workable approximations to be made of the amount of infiltrated water expected to be present in any given grid cell under various storm events.

These simplifying assumptions also have the advantage of allowing the probabilities associated with Atlas 14 rainfall events to be applied directly to the slope-failure model. That is, if it is assumed that all the rain is infiltrated during a rainfall event and water is not moving laterally in or out of a grid cell, then a probability of exceeding F (the minimum amount of infiltrating water that will cause failure) can be assigned for any rainfall event using the Atlas 14 data.

Studies show that most slope failures have occurred after soil has become saturated as a result of an extended period of rainfall. Because of this, consideration of rainfall events with durations longer than 24 hours was seen to be of most relevance for the slope-failure model. After testing the model by overlaying Atlas 14 data of varying storm durations, it was determined that the 3-day rainfall period would be the most useful for using the model to determine slope failure susceptibility.

Note that the temporal distribution of rainfall—the varying rainfall intensity that will occur during the course of a 3-day storm event—was not taken into account for the purposes of this modeling effort. Only the total rainfall amount for the 3-day event is used in the model.

CHAPTER 5: PROGRAMMING AND GIS ASPECTS

5.1 PROGRAMMING NEEDS

In order to calculate slope failure susceptibility results over a wide geographic area, the mathematical model needed to be incorporated into the framework of Esri's ArcGIS software. Processing the data required use of ArcGIS's Spatial Analyst extension.

After development of the mathematical model for slope failure (as presented in Section 4.0), code was written in Python to allow the model to be used within the ArcGIS environment. The scripting effort had the additional benefit of the development of user input screens, saving time through automation, and helping to ensure data quality and consistent results.

All model inputs were formatted as a file geodatabase raster and were "clipped" so as to have the same study extents, and modified as necessary so as to all be projected in the same coordinate system. The data from the SSURGO datasets come out of the Soil Data Viewer toolbar as a polygon, so they required manual conversion to raster format prior to being incorporated into the model.

Note that in some small portions of the mapped areas, NRCS soil map units are missing the needed soil-property information. This data deficit seems to occur most often in cases where the soil map units have been assigned non-specific names – for example, units labeled "steep land" in Scott County. To remedy this situation, prior to converting them to raster datasets the soils data were reviewed for missing values and the required information was then manually populated using information from adjacent soil units.

Determination of each soil's internal friction angle (φ) was necessary before it could be exported to a raster. The internal friction angle was determined by first creating a union between the USCS soil type polygon and the plasticity index polygon provided in the SSURGO dataset. Then, the USCS to φ lookup table was joined to the resulting union based on the USCS rating. The initial φ values were placed into a new field based upon the lookup. In the case of CL and CH (clayey) soils, the overriding φ values for clays were calculated based upon the equation (Terzaghi et al, 1996):

$$\varphi = 0.0014\ \mathrm{Ip2} - 0.2718\ \mathrm{Ip} + 35.41 \qquad \textbf{Equation 5.1}$$

In Equation 5.1, I_p is the plasticity index.

5.2 ADOPTION OF 5-LEVEL FAILURE SUSCEPTIBILITY INDICATOR SCHEME

The model output was initially reported as the total number of inches of precipitation over a 3-day period that would be necessary to instigate a slope failure. Because for slopes most susceptible to failure, it takes relatively little rain to trigger failure, the output had low numbers (of inches of rain) indicating high susceptibility to failure, and high numbers indicating low susceptibility. Although it was

correct and reflective of the modeling methodology, this reporting scheme was deemed to be confusing, so a different approach was developed.

The approach developed for the mapping involved using Atlas 14 data to represent modeled susceptibility results in five categories – from very high susceptibility to very low susceptibility. The susceptibility levels continue to be based on the likelihood of a given (3-day) precipitation event to occur in a given geographical area, with susceptibility levels reported for each location. The resulting slope-failure susceptibility levels are reported for each mapped grid cell as follows:

- *Very High Susceptibility* – for areas susceptible to failure as a result of events smaller than a 25-year event
- *High Susceptibility* – for areas susceptible to failure as a result of a 25- to 50-year event
- *Moderate Susceptibility* – for areas susceptible to failure as a result of a 50- to 100-year event
- *Low Susceptibility* – for areas susceptible to failure as a result of a 100- to 200-year event
- *Very Low Susceptibility* – for areas susceptible to failure as a result of a 200- to 1000-year event

Color coding is used (see map legends) to indicate the susceptibility levels on the maps generated by the GIS-based model.

This reporting scheme continues to reflect the fact that susceptibility to failure will be greater in situations where smaller rainfall amounts (for example, rainfall amounts that would be expected during the three-day storm that would occur relatively frequently – once every 25 years) might be expected to initiate slope failure. Conversely, susceptibility will be lower where the situation is such that larger rainfall amounts (such as those resulting from a 1000-year storm) would be expected to be needed to instigate slope failure.

The process of assigning a susceptibility category to the model output based upon the Atlas 14 precipitation frequency estimates was also automated through development of Python coding within ArcGIS. A new "susceptibility" raster output was created by comparing the original model ouput (in inches of precipitation) against the Atlas 14 precipitation frequency estimates.

(Note that the term *susceptibility*, rather than *risk*¸ has been used for the model results. After consultation with the TAP, it was felt that the term *susceptibility* was more appropriate in that it simply conveyed a sense of the likelihood of slope failure. *Risk*, by contrast, seemed to imply that property damages or injury may result from the slope failure, and the model has no means of registering this sort of harm. In this sense, *risk* would need to be determined by the facility owner – for example, the county engineer, city engineer, developer, etc.)

CHAPTER 6: CALIBRATION/VALIDATION PROCESS

6.1 GENERAL APPROACH TO CALIBRATION AND VALIDATION

For *calibration* of the model, it was also necessary to identify situations in which the LiDAR data had been collected prior to recent slope-failure events. In this way, one could see whether or not slope failure had actually occurred in locations where the model output (based on pre-failure slope conditions) was showing high susceptibility. Given the short history of LiDAR data, suitable areas for calibrating the model were limited. However, the slope failure sites along Highway 210 in Carlton County—resulting from the June 2012 storm event—were seen to be suitable for calibration.

Because there is inherent uncertainty regarding the site-specific accuracy of the SSURGO-provided soils data used in the model, it was initially assumed that certain soil parameters (i.e. effective cohesion) would need to be adjusted in order to properly calibrate the model. It was therefore seen as necessary to calibrate the model for areas in which the available soils data was as complete, so that the data could be closely examined and adjusted as necessary. The Highway 210 area had the additional advantage of having an abundance of soils data resulting from recent investigations of slope failures in the area.

However, model testing showed that calibration using adjustments of the standard values for soil parameters was in fact not needed to produce susceptibility indications that correlated well with known (subsequent) slope failures. As a result, no soil parameters were seen to require calibration. This made for considerable simplification in using the model.

The value of Z (soil layer depth) in Equation 4.2 could also be regarded as a calibration parameter. The SSURGO dataset provides soils information for depths up to six feet, so the soil layer depth could be set to a maximum value of six feet. However, Z values smaller than six feet could also be selected for the modeling. To evaluate which value of Z would be best suited for the modeling, the model was tested using Z values of 3, 4 and 6 feet. Testing showed that smaller values of Z resulted in slightly more areas being indicated as susceptible to failure, and gave predictions of slope failures occurring as a result of larger rainfall events.

The reason behind this can be explained as follows: As slope angle exceeds internal friction angle, the weight of soil is the critical factor for landslides during storm events. Therefore, a six-foot soil layer, being heavier, is more susceptible to failure than a 3-foot soil layer.

For soils with slope angles less than the internal friction angle, the weight of soil is no longer the critical factor, so a 3-foot soil layer may become more susceptible to slope failure than a six-foot layer. Nevertheless, in these lower-slope situations significantly more rain is required to cause slope failure; thus less frequent events cause failure.

These considerations suggested that the use of a Z of six feet as a basis for the slope-failure modeling would be more suited to the goals of this study. We have used a Z of six feet as the basis for the susceptibility mapping.

For model *validation*, the slope-failure sites recorded and georeferenced by MnDNR (Jennings et al, 2016) were used. The failure sites examined in the validation process were mainly located in Hennepin, Carver, Scott, Sibley and Winona Counties. Modeled slope-failure susceptibility predictions were compared with locations in these counties where slope failure was known to have actually occurred.

6.2 CALIBRATION OF THE SLOPE FAILURE SUSCEPTIBILITY MODEL ALONG HIGHWAY 210 IN CARLTON COUNTY

The GIS-based model was calibrated by focusing on a small study area of approximately 8 square miles in Carlton County (Figure 6.1). The calibration area included slopes adjacent to a portion of Minnesota State Highway 210 where landslides were known to have occurred after the intensive storm event of 2012. In this area, extensive studies and repairs are ongoing. The LiDAR survey had occurred in 2011, only a short time before the event, so that good pre-event and post-event aerial imagery is available.

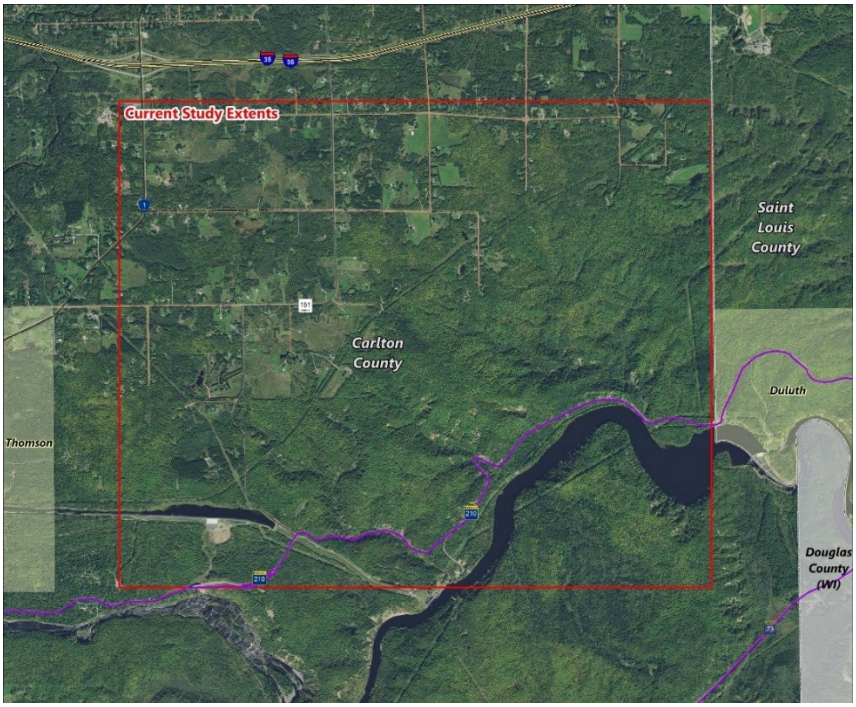

Figure 6.1 An area of approximately eight square miles in Carlton County that was used for model calibration

Figure 6.2 (left image) is the aerial imagery of a small section of the area, and shows slope-failures along Highway 210. Figure 6.2 (right image) shows the model results for those areas, with different levels of susceptibility to failure indicated through color coding. **Error! Reference source not found.** and Figure 6.4 show other stretches of Highway 210, with both observed and modeled slope-failure sites.

It has been noted that the model incorporates a relatively simple structure based on infinite-slope theory and utilizing the relatively low-resolution SSURGO dataset. Nevertheless, comparison of the pre-event modeled susceptibility indications with post-event aerial photography along Highway 210 show that the GIS-based model can predict areas susceptible to slope failure with reasonable accuracy.

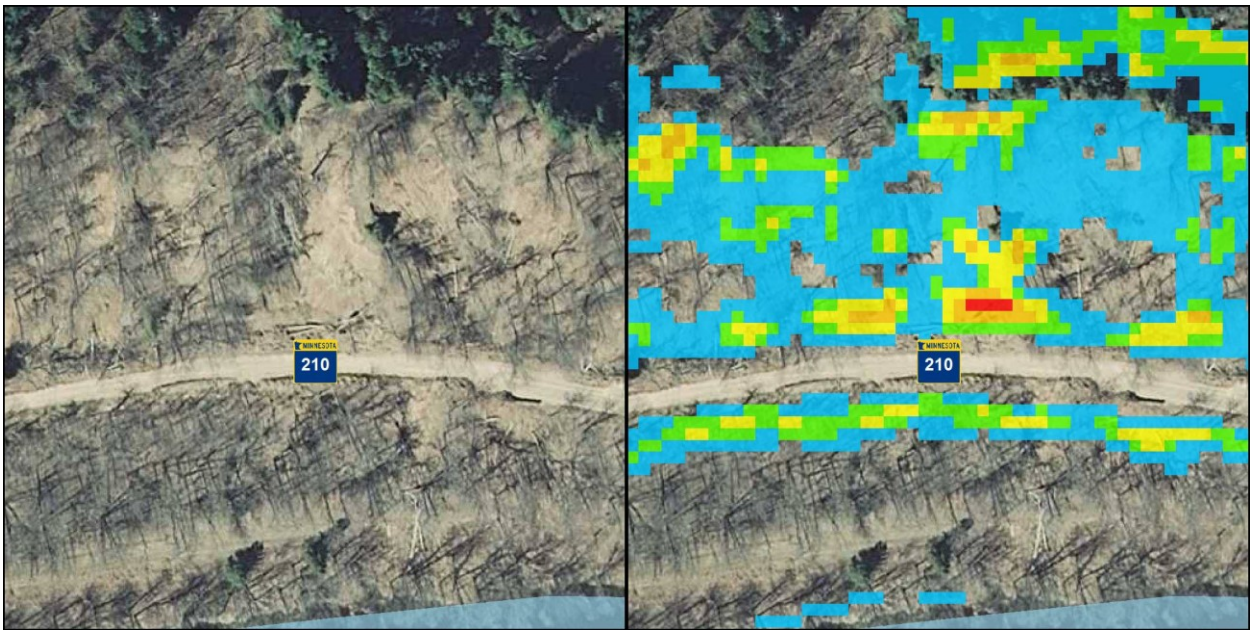

Figure 6.2 *Left:* Aerial photo of a slope-failure site at mile post 225 along Minnesota Highway 210 in Carlton County. *Right:* GIS-based model results for the same location. Color-coding shows levels of failure susceptibility, with red being very high and blue being very low.

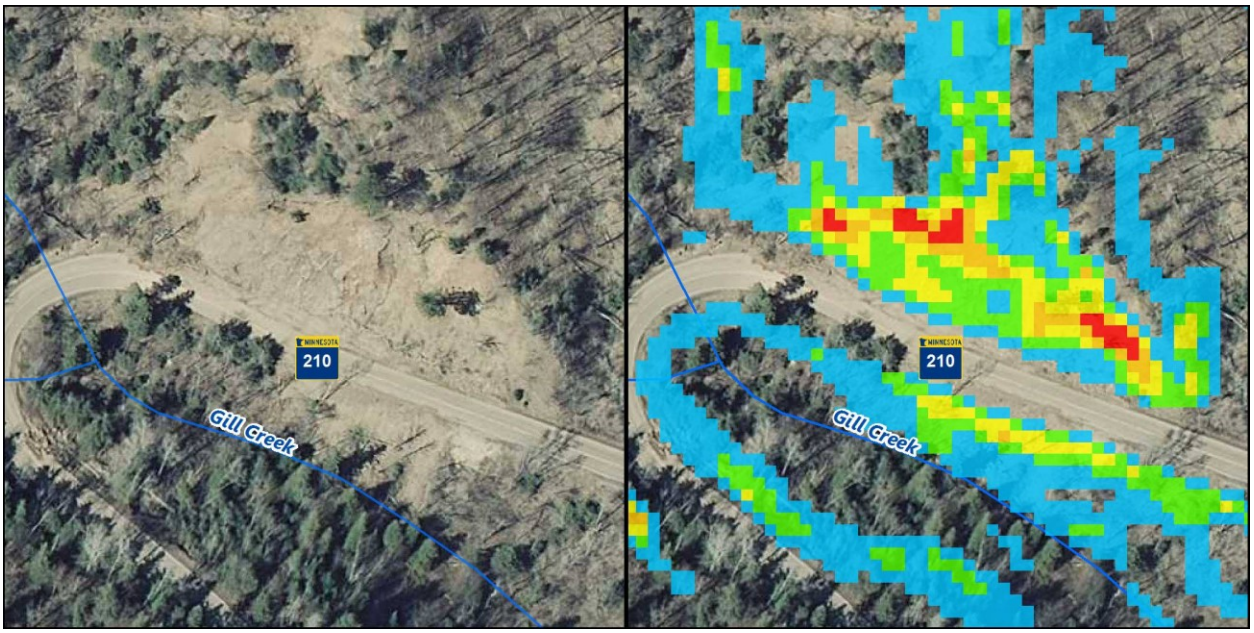

Figure 6.3 ***Left:*** **Aerial photo of a slope-failure site at mile post 224 along Minnesota Highway 210 in Carlton County.** ***Right:*** **GIS-based model results for the same location. Color-coding shows levels of failure susceptibility, with red being very high and blue being very low.**

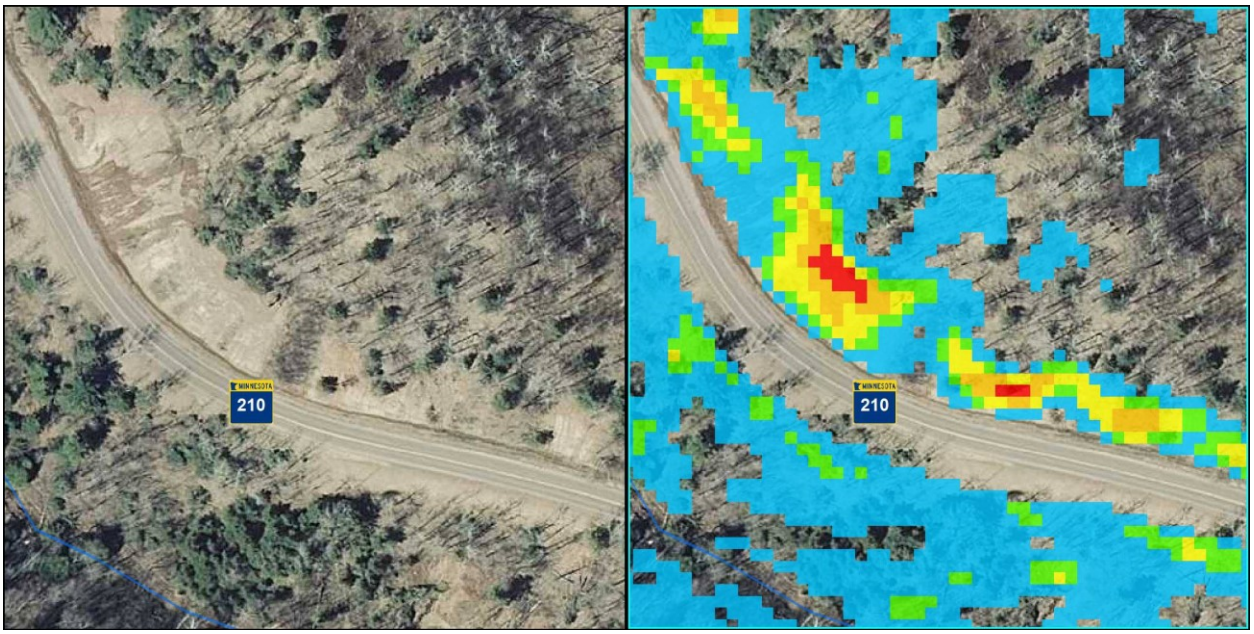

Figure 6.4 ***Left:*** **Aerial photo of a slope-failure site at mile post 223 along Minnesota Highway 210 in Carlton County.** ***Right:*** **GIS-based model results for the same location. Color-coding shows levels of failure susceptibility, with red being very high and blue being very low.**

6.3 VALIDATION OF THE SLOPE-FAILURE SUSCEPTIBILITY MODEL IN SIBLEY, SCOTT AND CARVER COUNTIES

The failure sites listed in the MnDNR inventory used for validating the model occurred at various times across the past 100 years. Some imprecision in the geographical locations given for the slope failures may be expected, given that in many cases the locations are based on historical and newspaper reports. And a review of the reported coordinate data for these slope failures suggests that many of the reported locations must be approximate. This made use of the historical slope-failure data somewhat difficult.

Nevertheless, the GIS-based model's predictions showed good correlation with at least some of the MnDNR-listed failure sites in selected areas in Sibley, Scott, and Carver Counties. Figure 6.5 through Figure 6.8 compare the aerial imagery with the GIS-based model results.

Overall, the validation process confirmed that the GIS-based model is a useful tool for identifying areas susceptible to slope failure.

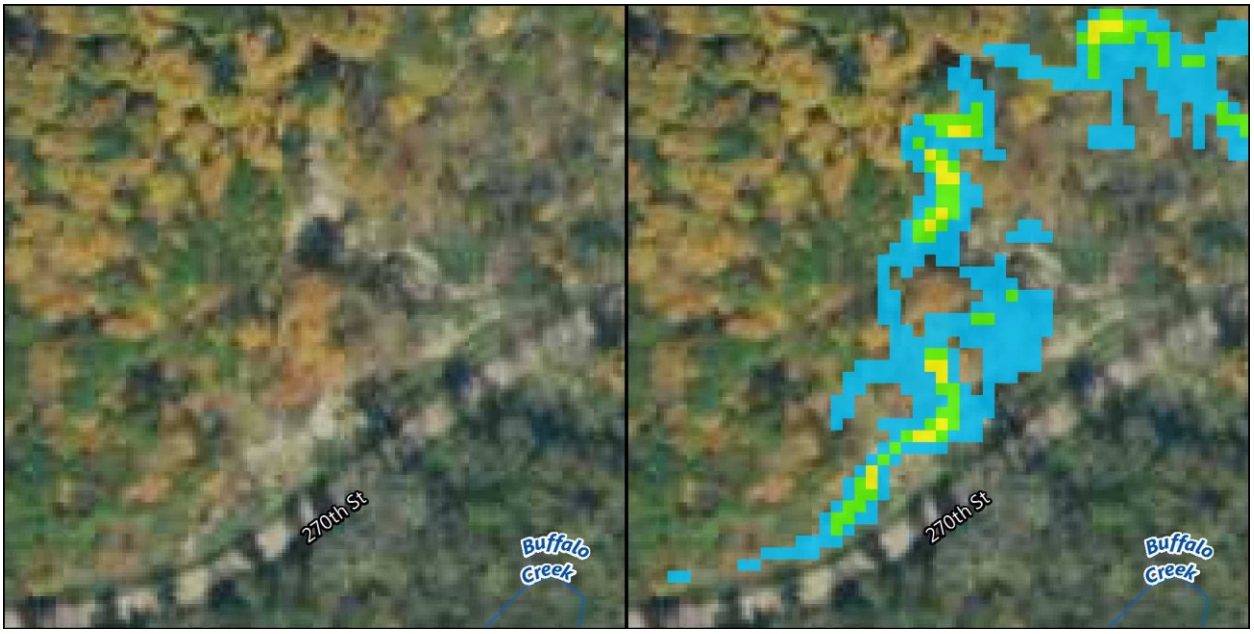

Figure 6.5 *Left:* Aerial photo of an old slope-failure site along 270th Street in Sibley County.
***Right:* GIS-based model results for the same location. Color-coding shows levels of failure susceptibility, with red being very high and blue being very low.**

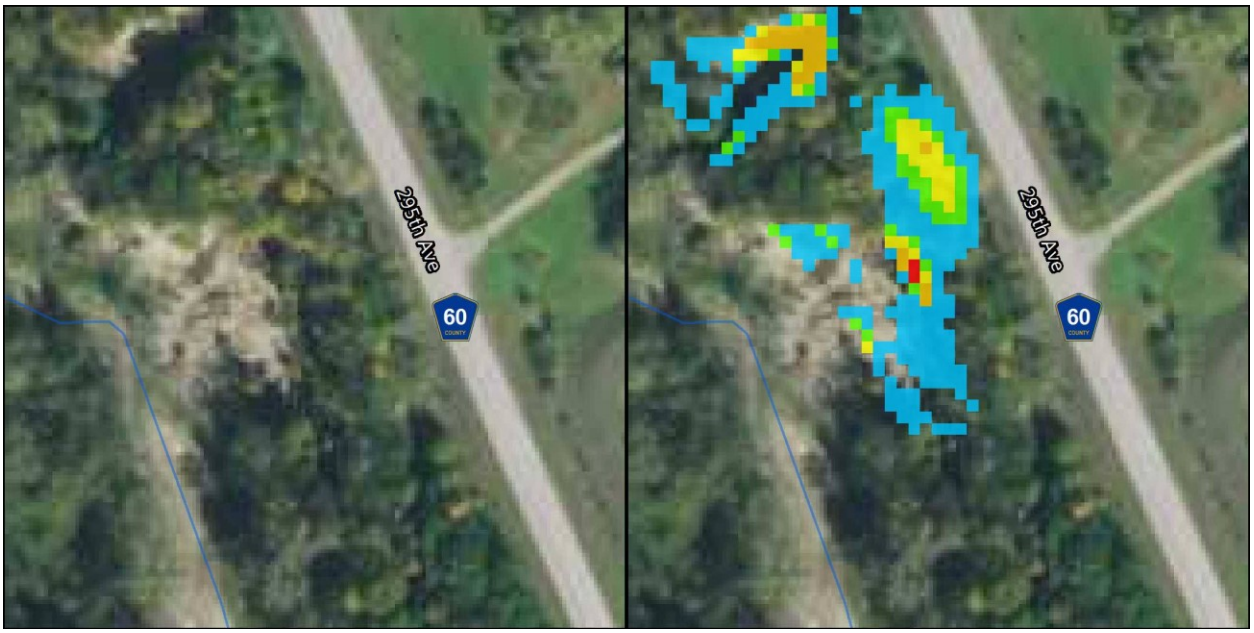

Figure 6.6 ***Left:*** **Aerial photo of an old slope-failure site along 295th Avenue in Sibley County.**
Right: **GIS-based model results for the same location. Color-coding shows levels of failure susceptibility, with red being very high and blue being very low.**

Figure 6.7 *Left:* Aerial photo of a slope-failure site in agricultural area near Stoppelmann Blvd and US 169 (southeast of Belle Plaine), Scott County. *Right:* GIS-based model results for the same location. Color-coding shows levels of failure susceptibility, with red being very high and blue being very low.

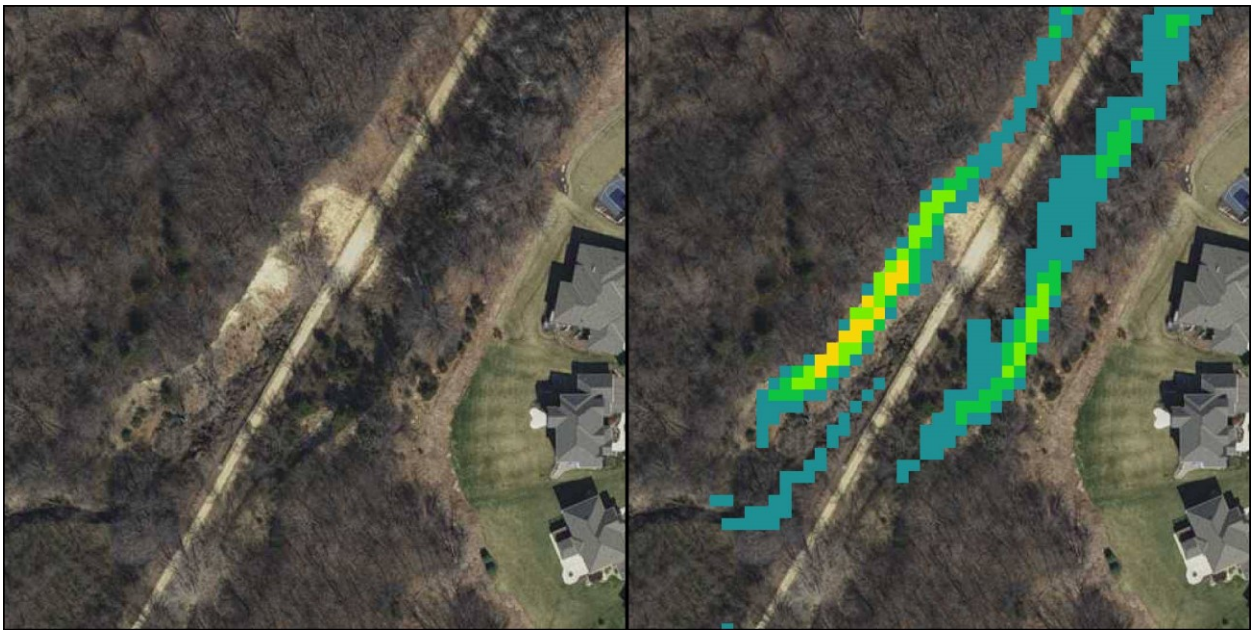

Figure 6.8 *Left:* Aerial photo of a slope-failure site along Minnesota River Bluffs Trail, Chanhassen, in Carver County. *Right:* GIS-based model results for the same location. Color-coding shows levels of failure susceptibility, with yellow being medium and blue being very low.

CHAPTER 7: GEOTECHNICAL REVIEW AND HYDROLOGIC REVISION

After developing the maps based on equations presented in Section 4.0, Barr was asked to consider possibilities for refining its GIS-based slope-failure model. Barr was to revisit the project approach after re-examining the geotechnical and hydrologic aspects, and considering the possibility of utilizing other available and relevant data. The intention was to look for possible refinements and improvements to the original approach.

In the search for refinements, three geotechnical experts reviewed the first draft of this report and provided feedback and suggestions for possible improvements. Additional work was also done to determine if available MnDOT soil boring data could be utilized in the current GIS-based model. Finally, the hydrologic aspects of the model were re-examined to determine if improvements could be made to the approach to assessing slope failure risk.

Section 7 summarizes the results of this additional work.

7.1 GEOTECHNICAL REVIEW

Summaries of the three geotechnical reviews are provided in Appendix B. The key points of the overall geotechnical review are as follows:

1. The underlying methodology appears sound for its intended use, especially considering the need to rely on generally-available datasets. All reviews indicated support for the model's reliance on the infinite-slope theory and equations as the basis for making probabilistic evaluations of the likelihood of the shallow slope failures that would be expected to result from large rain events.

2. The reviews pointed out that within the model, slope failure occurs as a result of rainfall-induced changes in soil cohesion. Because of this, it was suggested that efforts to improve the model should focus primarily on improving the model's treatment of surface water hydrology and infiltration.

3. The reviews resulted in a closer examination of certain soil parameters (specifically cohesion, effective cohesion, soil suction, and friction angle) may be warranted. Also, it was pointed out that it should be made explicit that the model begins with an assumption of "drained" conditions within the upper (six-foot) soil layer.

4. It was also noted that the effects of vegetation on a slope are variable and both type and site-dependent. Therefore, they agreed that the model should not attempt to incorporate vegetative effects on slope stability, and that the report should be explicit in noting that such effects are not accounted for in the model.

5. It was suggested that because past failures are known to be reliable predictors of proximal future failures, it would be helpful to find a way to make use of historical slope-failure data, where it is available.

Items 1 and 5 supported the basis of the approach used originally for the slope-failure model developed for this project. Items 2, 3 and 4 resulted in improvements to the approach to how the model deals with soils and hydrology. Item 4 was noted and the disclaimer is now included as part of this report.

The geotechnical review suggested a need to focus more closely on soil cohesion. As discussed in Section 7.3, it was determined that given the use of the infinite slope stability theory along with the SSURGO data set, if the soil cohesion is not included in the model, many areas will be assessed as being unconditionally unstable. In addition, the model also showed that the assumption of a cohesion value of zero for some soil types, as shown in Table 4-1, will result in the prediction of landslides during smaller storm events even in areas with mild slopes. As a result a small nominal value of cohesion of 2 to 10 kPa can provide realistic results for the area highly vegetated and stable.

7.2 USE OF MNDOT SOIL BORING DATA

MnDOT soil borings are generally logged as one of two types. *Roadway borings* are typically performed for the primary purpose of determining soil type/classification and index properties. MnDOT roadway borings data is stored in a Microsoft Access database. Roadway borings are inventoried by the MnDOT Materials Units – logs are generated in short-form text reports coming from the database.

Foundation borings are performed for the additional purposes of collecting quality soil samples and determining detailed engineering properties. Foundation boring data is processed and boring logs are prepared using software called gINT® developed by Bentley. Foundation borings performed by MnDOT or engineering consultants are inventoried by the MnDOT Foundations Unit as either gINT project files, PDF-formatted files, or image (i.e. TIFF) files. Therefore, any use of MnDOT boring data in the model would require that the model be equipped to deal with a variety of soil data file formats.

Historically, MnDOT has not used the USCS for classifying soils on either roadway or foundation boring logs. Instead, MnDOT has used a modified triangular textural classification system (similar to that of the USDA). The MnDOT system is based solely on the relative ratios of sand, silt, and clay in the soil. By contrast, the USCS also incorporates soil plasticity and ratio of gravel-sized particles. As the current landslide susceptibility model is based on USCS soil types, any use of MnDOT boring data would require developing an algorithm to convert the soil type information from the less precise MnDOT system into USCS.

Soil borings are typically performed using drill rigs mounted on trucks or on tracked all-terrain vehicles. These rigs require sufficiently flat ground in order to level the rig and drill a vertically plumb borehole. In other words, soil borings are not typically performed along steep grades that would be susceptible to failure. There is therefore little chance that soil boring data would be very useful in ascertaining the soil

conditions on nearby slopes susceptible to failure. Furthermore, soil borings represent discrete points of information. The density of boring locations that would be required to be of statistical significance in the model's areal mapping is not likely to exist except in very rare cases.

In summary, examination of the possibility of utilizing available soil boring data showed that the available data is not likely to be practical or useful for this project.

7.3 HYDROLOGIC REVISION

The hydrology of the current GIS-based model was re-examined, and the main weaknesses of the original model were determined to be as follows:

1) The critical depth of water was assumed to be the depth of a rainfall event. Because of the broad application of the GIS-based model, a simplifying assumption was made that all rainfall is infiltrated into the soil to the depth of the plane of failure before any surface runoff would occur.

2) The contributing drainage area to a cell was not considered in determining the water conditions in the soil prior to a rainfall event.

3) Water loss from the soil column due to groundwater flow parallel to the failure plane was not included in the GIS-based model. In essence, the model assumed that the entire amount of rainfall from the rain event would infiltrate, and no water would flow out of a given cell during the rainfall event.

4) The duration of the critical storm event was assumed to be three days, and no other event durations were considered in assessing the susceptibility of a slope to failure.

The approach to dealing with each of these weaknesses is as follows:

Item 1 relates to assumptions about infiltration. Infiltration is closely related to the particular soil characteristics, and to the initial moisture condition in the soil. The initial moisture condition can be assumed to be at about field capacity, or some nominal moisture content based on average annual precipitation and evapotranspiration in a region. The model can significantly improve to account for the amount of infiltration during storm events. Since the probability of failure depends on the Atlas 14 precipitation amounts, the duration of those events can be included in estimating the depth of infiltration (I.e., the seepage rate). Infiltration can be approximated using a more complex method such the Green-Ampt method or a simple method like the ϕ-index method. Based on some preliminary trials, it was concluded that even a simple ϕ-index method improves the results.

Item 2 focuses on lateral movement of infiltrated water. The possibility of improving the model by incorporating lateral water movement was tested by modifying the initial conditions of the soil prior to

rainfall events. Testing involved using a general wetness condition for a cell based on mean annual rainfall. It was determined that an initial moisture condition wetter than field capacity could result in better determination of slopes susceptible to failure worth further investigation.

Regarding item 3, we determined that having good groundwater data for a particular area of concern would be expected to improve the model in identifying areas which are susceptible to failure. This data, when and where available, could be incorporated in future model modifications.

In considering item 4, a three-day duration for rainfall events was indeed seen to be arbitrary, and therefore attempts were made to determine the *critical duration* of storm events (i.e., the storm duration that would cause slope failure). To determine the critical storm duration, the method proposed by D'Odorico et al. (2005) was utilized. However, the method was modified and then applied sample data in a spreadsheet model (for more information on the approach, see Appendix C). Incorporating the approached proposed by D'Odorico et al. (2005) removes the arbitrary 3-day duration and provides a more realistic probability of failure. However, the approach should incorporate an infiltration model as discussed in item 1. Figure 7.1 shows the results obtained using the modified model for estimating the critical duration of storms. The left panel is a hill shade map of an area projected over its aerial photo. The right panel shows the critical duration of storm events that can result in slope failure for each particular location. It can be seen that critical duration is a function of both soil type and slope. In this example, the critical duration varies from one hour to twelve hours.

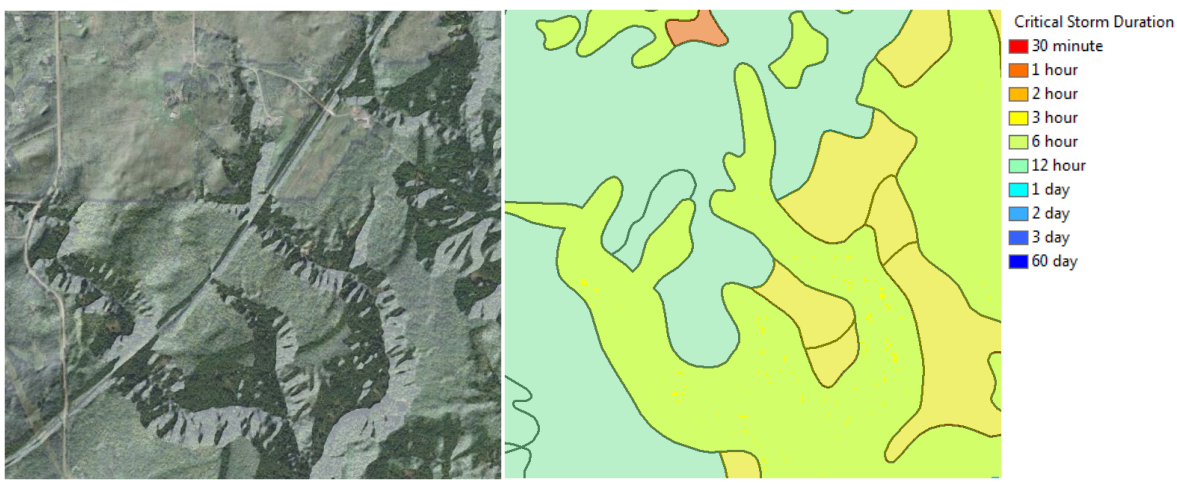

Figure 7.1 *Left:* Aerial photo with hill shading for a sample area in Minnesota. *Right:* GIS-based model results for the same location. Color-coding shows critical duration of failure susceptibility during critical storm events.

CHAPTER 8: RESULTS AND APPLICATIONS

8.1 RESULTS

Examples of the slope-failure susceptibility mapping developed through work on this project were presented in Section 6.0. Statewide mapping has been prepared for two counties – Carlton and Sibley. To examine the mapping results in a way that is useful, it's necessary to zoom in closely on the area in question. For that reason, it is impractical to present the maps in printed format. Therefore, the statewide mapping results have been provided (separately) in the form of PDF files for which the viewer can vary the field of view to a scale that is convenient and helpful.

A series of large-format maps at 1-inch=500-foot scale was created for both Carlton and Sibley Counties. The counties' extents were divided into a grid of equally sized map sheets and assigned alpha-numeric labels. Both Carlton County and Sibley County were mapped using only 0 to 6-foot soils depth range. Carlton County map sheet C-10 (Appendix D1), and Sibley County map sheet D-10 (Appendix D2) are provided as examples of what can be seen on the large-format maps. (The complete map series is provided for the TAP via an FTP site; access instructions have been provided separately.)

Due to variations in each county's topography, no model results are provided for some large (and mostly flatter) areas of the two counties. These areas were either unconditionally stable or the precipitation required to initiate a slope failure would be greater than that of the Atlas 14 1000-year rain event. Similarly, map sheets showing slope-failure susceptibility in only a few in only very small areas—at locations of gravel pits, construction activities, agricultural ditching, and other similar anthropogenic geographic features – were also not provided.

As has been mentioned previously, relative level of susceptibility to failure is indicated through color-coded highlighting of the slopes. The five levels of susceptibility to failure are indicated on the map legends. The highlighting provides a way for the viewer to easily identify portions of a county that have a concentration of highly susceptible slopes.

As can be seen when viewing the maps, and as would be expected, the susceptibility to slope failure varies greatly from location to location, and from general region to general region within each county. It can also be seen that there are locations where failure-prone slopes would be of more concern than others. For example, many of the slopes identified as failure-prone are not adjacent to vulnerable structures, infrastructure, or sensitive ecological features.

However, in some areas potential slope failure may pose greater concerns. Those areas of the maps can be examined more closely to determine where there may be slopes that need further attention—areas in which slope failure might result in significant inconvenience, damage, or even loss of life.

8.2 APPLICATIONS

The results of this project have the potential to assist local and state engineers and managers in improving road safety. The mapping provided may provide useful information by which, for example, local road engineers can identify susceptible areas that need further attention and study. Preventative measures might be taken as a result—slopes might be stabilized, retaining walls might be put in place, drainage might be diverted, adjacent infrastructure might be protected, etc. Such preventative measures have the potential to protect the public and avoid costly damages.

Even if preventative measures are not taken, knowledge of the existence of susceptible areas may improve emergency preparedness plans. Plans and preparations can be generated, and funding reserved for providing quick and effective cleanup and repairs. The mapping might be also help highway maintenance crews be more aware that slope failures are likely in certain areas when large rainfall events are expected—thus allowing for better preparation and reduced response times should a slope failure occur.

It may also be that state, county, and local highway departments are able to use the slope-failure susceptibility model to conduct screening during the planning phase of a project in areas where slope failure is thought to be of concern. In areas of higher susceptibility, preventive measures (involving, for example, water management in the watershed at the top of the slope) could be undertaken to ensure the long-term viability of newly or re-constructed sections of roads.

In cases where slope failure has occurred and repairs are necessary, the slope failure susceptibility mapping may assist highway engineers in justifying FHWA betterment funding. If, for example, it can be shown that the damaged road is in an area of high susceptibility, emergency relief funding may include funding for betterments that will help prevent recurring damage to the roadway and/or avoid future slope failures.

Provided that the results of this project are seen as beneficial, additional and related work may be indicated. This might include:

- **Extension of the mapping to the remaining counties in Minnesota** – Only two counties have been mapped so far, and it is likely that engineers and managers in the remainder of Minnesota's counties would benefit from applying the slope-failure model and developing mapping on a broader scale. An additional benefit resulting from extending the model's application is that greater experience with the model may help point the way toward further refinements that could improve its accuracy. It may also provide the opportunity for developing methods of automation that would reduce the necessity for manual editing of the SSURGO data.

- **Associated mapping of vulnerable features** – It may be helpful to identify and map vulnerable features and structures near or adjacent to susceptible slopes. In addition to roads, features and structures of concern may include sensitive ecological features, transmission lines and pipelines,

residential and commercial buildings, bridges, culverts, etc. Mapping these structures would be of assistance to local engineers and managers in determining which of the susceptible slopes need the most attention.

- **Consequence analysis** – An extension of the mapping of vulnerable features would be to conduct consequence analysis and mapping. This effort would take into account the proximity of vulnerable features, but also the degree to which they are vulnerable should slope failure occur and the relative importance of protecting them. This analysis would allow further focusing of preventative or remedial measures.

- **Development of risk-based approach for making slope-failure protection decisions** – A variety of approaches to dealing with the risk of slope failure exists, and each has its own advantages, drawbacks, and costs. A risk-based decision algorithm might be developed to assist engineers and managers in determining which approach or approaches might be best suited to dealing with the threat of slope failure. The algorithm would take into account factors such as steepness, subsurface geology, soil type, local drainage considerations, consequence analysis, and cost.

CHAPTER 9: SUMMARY AND CONCLUSIONS

Through work on this project, we have developed a conceptually simple slope susceptibility-failure model that relies on generally accepted geotechnical theory. The model has the advantage of utilizing only publicly statewide available data; no local field investigations or data acquisitions are needed. Because it is GIS-based, the model provides results in a readily accessible map-based format. The color-coded susceptibility highlighting on the maps makes it easy to identify areas of concern.

We tested the model to see whether its predictions match up well with locations in which slope failures are known to have occurred. Generally the results of this testing are encouraging. While the model is not intended to be (and should not be) used to determine whether or not a slope will fail in a particular location, the testing allows confidence that the model is, in fact, giving a good indication of where there are areas where slope failure should be of particular concern. Subsequent work on the model may provide opportunity for additional refinements that might further enhance its specificity and predictive ability.

It is our hope that the model will prove useful as a screening tool that would allow state and local engineers and managers to become aware of areas of higher susceptibility. Such areas would be further investigated "on the ground" to determine whether the model's conceptual assessment of slope-failure susceptibility matches up well with location-specific conditions. State and local officials may thus be able to more effectively plan mitigation measures to avoid costly damages in locations where field investigations confirm that slope-failure susceptibility is high.

Further refinement of the model, e.g., incorporating a module to estimate infiltration and estimating critical duration of storms with different annual exceedance probability, is likely if funding allows the susceptibility mapping to be extended to the rest of the counties in Minnesota. The inclusion of at-risk structures in the mapping may also enhance the model's utility. The model may also be applied in slope-failure consequence analysis to better allow managers to focus on areas of high concern. A further application might involve the development of guides or algorithms to assist local managers in planning mitigation or emergency response measures for locations in which slope failure is seen as likely.

We are pleased to have had the opportunity to work on this challenging and interesting project, and we are grateful to the LRRB and the members of the TAP for their support and encouragement along the way. We look forward to further collaboration in extending the use and increasing utility of the model.

REFERENCES

Casadel. M., Dietrich, W.E., and Miller, N.L. 2002. "Testing a Model for Predicting the Timing and Location of Shallow Landslide Initiation in Soil-Mantled Landscapes." *Earth Surface Processes and Landforms.* **28**, 925-950.

D'Odorico, P., Fagherazzi, S., and Rigon, R. 2005. "Potential for landsliding: Dependence on hyetograph characteristics." *Journal of Geophysical Research.* 110, F01007, doi:10.1029/2004JF000127.

Duncan, J. M., and Wright, S. G. 2005. *Soil Strength and Slope Stability*. Hoboken, NJ. John Wiley and Sons.

Iida, T. 2004. "Theoretical research on the relationship between return period of rainfall and shallow landslides." *Hydrological Processes.* **18**, 739-756.

Jennings, C.E., Presnail, M., Kurak, E., Meier, R., Schmidt, C., Palazzolo, J., Jiwani, S., Waage, E., and Feinberg, J.M. 2016. *Historical Landslide Inventory for the Twin Cities Metropolitan Area.* St. Paul, MN: MnDNR

Montgomery, D. R., and Dietrich, W. E. 1994. "A physically based model for the topographic control on shallow landsliding." *Water Resources Research.* **30(4)**, 1153-1171.

Minnesota Pollution Control Agency. 2017. *Minnesota Stormwater Manual*. St. Paul, MN: MPCA

Okimura, T., and Ichikawa, R. 1985. "A prediction method for surface failures by movements of infiltrated water in a surface soil layer." *Natural Disaster Science*, **7(1)**, 41-51.

Rosso, R., Rulli, M. C., and Vannucchi, G. 2006. "A physically based model for the hydrologic control on shallow landsliding. *Water Resources Research.* 42, W06410, doi:10.1029/2005WR004369.

Terzaghi, K., Peck, R. B., Mesri, G. 1996. *Soil Mechanics in Engineering Practice.* New York, NY. John Wiley & Sons, Inc.

Winterkorn, H. F. and Fang, H. 1975. *Foundation Engineering Handbook.* New York, NY. Van Norstrand Reinhold Company.

APPENDIX A

LITERATURE REVIEW

resourceful. naturally.
engineering and environmental consultants

BARR

Memorandum

To: Paul Stine, Farideh Amiri;
Blake Nelson, Joel Ulring, Philip Schaffner, Mike Tardy, Jake Balk and Tim Becker
From: Omid Mohseni, Charles Hathaway, Greta Backman, Michael Hochscheidt, Leslie DellAngelo, and Aaron Grosser
Subject: Slope Failure Risk Analysis – Summary of Literature Review Findings
Date: August 26, 2016
Project: 23621218

1.0 Introduction

This memo summarizes the findings of a literature review conducted as part of the slope failure risk analysis research project we have undertaken for the Local Road Research Board (LRRB). The purpose of the literature review was to survey the range of available information regarding landslide susceptibility. In this memo, previous studies are identified, summarized, and cataloged. We have also identified information and causative factors that appear to be relevant to landslides in Minnesota.

This memo is organized as follows: Section 2.0 summarizes the general approach of the literature review, Section 3.0 is a brief summary of available research and study methodologies, Section 4.0 outlines the major relevant causative factors of landslides identified through this literature review, and Section 5.0 is the list of reviewed papers and reports, and includes a short description for each document.

2.0 Approach

Given the limited scope of the present study for LRRB, a comprehensive review of all available literature could not be undertaken. Therefore, we focused on studies that appeared to have application to Minnesota (i.e., studies done in areas with similar geography, landscapes and climate), and that were conducted by government agencies such as state transportation departments and the US Geologic Survey. We attempted to identify and examine the most-referenced papers in this field, as well as papers that described studies with aims similar to those of this project.

3.0 Summary of Research Available for Use

Our review of the literature reveals that the creation of landslide, debris flow and/or slope failure occurrence inventories is common practice in many regions of the world. In addition, many studies have been conducted that attempt to quantify the likelihood of the occurrence of landslides or identify areas that have the propensity to produce these phenomena.

However, landscape processes and triggers tend to be unique to a specific geography. As a result, only a small number of reviewed studies seem to have applicability for Minnesota. Despite this limitation, the published studies provide valuable information on methods of analysis that may be used for this project.

3.1 Inventories

The first step in most landslide and slope failure susceptibility studies is compiling an inventory of historical slope failures. Landslide processes have been found to have a legacy effect – landslides follow landslides. Therefore, inventories of past failures can be used to determine where future failures are likely, based on spatial and temporal information.

The utility of landslide inventories is limited because that they tend to over-report landslides in developed areas, and tend to focus on recent landslides. And although a given geographic area may not have documented historic landslides, it may still be susceptible to landslides. Attempts are being made to increase the size of historical landslide databases by utilizing LiDAR data to identify failures based on ground surface morphology.

In Minnesota, the Department of Natural Resources (MDNR) has recently completed a study to inventory historical failures in the Twin Cities Metropolitan area using a variety of archival records. These records span the period from 1979 to 2014. Reportedly, the MDNR intends to complete a more comprehensive, state-wide inventory at some point in the future.

3.2 Susceptibility Analysis

Many landslide susceptibility studies have been published, and both qualitative and quantitative approaches have been applied. The most common approaches can be grouped into four categories: (1) geomorphic hazard mapping, (2) index-based methods, (3) statistically based methods, and (4) physically-based methods.

- Geomorphic hazard mapping of landslide susceptibility is a qualitative method that uses subjective expert judgement to identify actual and potential slope failures.
- In index-based methods, spatial distribution of causative factors are identified and their influence on observed failures are weighted.
- In statistical methods, multivariate statistical techniques are used to develop function relationships between causative factors and observed failures.
- Physically-based methods apply process-based geotechnical models, like the infinite slope model, to evaluate failure conditions from a set physical parameters.

It is important to note that most of these studies lack proper validation of the results (Aydilek and Ramanathan, 2013).

4.0 Major Causative Factors

The review of literature conducted for this study suggests that there is a finite list of major causative factors of landslides and slope failure relevant for Minnesota. These factors are summarized below. Note that because the factors influencing slope failure are unique to a particular location and set of circumstances, it cannot be said that any of the factors is universally more important than the others.

Slope angle

Other factors being equal, steeper slopes are more prone to landslides and slope failure than shallower slopes. A number of studies have identified slope angle ranges where landslides are most likely to occur for a given geography. However, other studies have shown that slope angle alone is not sufficient to gauge how vulnerable an area is to landslides. Other factors can cause a relatively steep slope to be stable, while a relatively shallow slope may be landslide prone.

Soil Type and Geology

The geotechnical properties of a soil (shear strength, permeability etc.), are significant factors in determining landslide susceptibility. Soils with a high shear strength are less susceptible to landslides than soils with a lower shear strength. The hydraulic soil properties of the soil are also important because these properties affect what intensity and duration of rainfall event is required to initiate a landslide.

Vegetation

At least one of the papers reviewed observed a correlation between vegetation and landslides, with the majority (56%) of landslides in the study area (Maryland) occurring in areas with low to medium-density grass. As discussed by Duncan and Wright (2005), woody vegetation (trees and large shrubs), provide mechanical reinforcement to the soil, as well as reducing infiltration and providing erosion protection and generally helping to protect against shallow sliding.

Land Use and Drainage Density

Characteristics of the drainage area at and above a slope – including drainage density and land use changes – are related to the geomorphology of a landscape. Drainage density calculations provide an estimate of the area prone to soil saturation, which is a major factor of slope failure.

Antecedent Precipitation/Soil Moisture

In many climatic regions, antecedent precipitation has been found to be related to occurrence of slope failures. Cumulative rainfall threshold relationships have been developed for specific geographies. These relationships are defined by parameters such as the total rainfall amount during the past 3 days, and the total rainfall amount during the previous 15 days (Seattle, Washington area); or the 1, 2, 7, 30, and 90-day antecedent precipitation (southwest United Kingdom).

Other studies have attempted to couple hydrologic models with simple slope-stability models to predict locations of shallow landslides. The hydrologic models are used to calculate soil saturation based on

contributing drainage area, soil transmissivity, and local slope. Then the "infinite slope stability model" (often used in slope stability evaluations) is used, with degree of soil saturation as an input parameter.

Rainfall Intensity and Duration

Many studies have found rainfall intensity and duration to be related to occurrence of slope failures. Empirical intensity-duration (ID) threshold relationships have been developed to try to identify conditions under which failures would be initiated. Many of these ID thresholds are unique to the climatic regions for which they were developed. However, global ID thresholds have been developed by normalizing the precipitation data by the mean annual precipitation and the "rainy-day normal" (which is the ratio of the mean-annual-precipitation to the average number of rainy days in a year).

5.0 List and Brief Summary of Reviewed Papers

Below is a chronological listing the papers we reviewed, along with a brief description of each document.

Montgomery, D.R. and Dietrich, W.E. (1994). A physically based model for the topographic control on shallow landsliding.

Montgomery and Dietrich (1994) discussed the combination of a contour-based, steady-state hydrologic model and a simple slope-stability model to predict the locations of shallow landslides. They used the hydrologic model TOPOG (O'Laughlin, 1986) in their study. TOPOG uses steady-state rainfall and maps soil saturation based on contributing drainage area, soil transmissivity, and local slope. The infinite slope stability model for cohesionless soils was used with the soil saturation from TOPOG as wetness parameter.

Carrara, A., Guzzetti, F., Cardinali, M., Reichenbach, P., (1999). Use of GIS Technology in the Prediction and Monitoring of Landslide Hazard.

Carrara et al. (1999) provided methods to use GIS software for predicting landslides. The authors argued that properly using GIS software to produce a hazard map requires an appropriate data set as well as appropriate expert analysis. The authors described how GIS is capable of analyzing several different types of failures (i.e., rotational and infinite slope) simultaneously because both analyses rely on the same data set. One of the largest difficulties, and largest costs, in creating this type of analysis (again, according to the authors) is collecting the required data. The authors argued that even if the required data collection is possible, the resolution of the data will likely be very coarse.

Guzzetti, F., Carrara, A., Cardinali, M., and Reichenbach, P. (1999). Landslide hazard evaluation: a review of current techniques and their application in a multi-scale study, Central Italy.

Guzzetti et al. (1999) discussed the most commonly used hazard evaluation methods. Then they discussed GIS-based models and the results of testing the methods in central Italy.

Iverson, R. M., (2000). Landslide Triggering by Rainfall Infiltration.

Iverson (2000) investigated the relationship between slope failure and landslide motion to groundwater pressure heads that change in response to rainfall. A response function was developed that predicts the

pressure head response to rainfall given input of the normalized time (which is normalized to the diffusivity of the soil and the thickness of the soil layer). The pressure head response to rainfall is the factor that governs slope failure and post failure landslide motion.

Laprade, W.T., Kirkland, T.E., Nashem, W.D., and Robertson, C.A. (2000). Seattle Landslide Study.

Laprade et al. (2000) provided a landslide study/evaluation that was conducted for Seattle Public Utilities (SPU) in response to landslides during the winter of 1996/97. A database was created with 1,326 landslides with the following information: location, date, type, geologic conditions, and possibly contributing factors.

Slope instability improvement recommendations were also presented for the different types of slides, including surface water improvements, groundwater improvements, retaining structures, soil reinforcement, grading, catchment structures, and diversion structures. The roles of vegetation, utilities, and roads in landslides are also discussed.

Cho, S.E., and Lee, S.R., (2002). Evaluation of Surficial Stability for Homogeneous Slopes Considering Rainfall Characteristics

Choe and Lee described that rainfall-induced landslides are typically caused by the loss of matric suction near the surface due to the saturation of surface soils. They described a method proposed by Pradel and Raad for estimating these types of slope failure. In order for a rainfall-induced landslide to be produced, the rainfall intensity must be greater than the infiltration capacity and the rainfall duration must be greater than a minimum time period. The authors stated that knowing this, as well as the soils' hydraulic characteristics, it is possible to produce a rainfall intensity curve that defines a rainfall event with the potential to produce landslides.

Chau, K.T. Sze, Y.L., Fung, M.K., Wong, W.Y., Wong, E.L., Chan, L.C.P., (2003). Landslide Hazard Analysis for Hong King Using Landslide Inventory and GIS.

Chau et al. (2003) developed a landslide hazard map of Hong Kong using GIS software. The most basic version of the hazard map was based on historic landslide records. Other factors such as geology, geomorphology, lithology, hydrology, vegetation and climate were eventually added to the GIS analysis. This paper highlights that GIS software can be used to correlate landslide occurrence to other variables (geotechnical properties, rainfall, etc.). The most robust landslide hazard maps will include multiple variables when calculating landslide risk. Which variables give the best correlation for landslide prediction, however, is not universally agreed upon. The methodology for this paper attempted to assign each variable included in the weighting factor. By summing the weighting factors, it was then possible to calculate the total landslide risk for a given area.

Schulz, W. H., (2004). Landslides Mapped Using LiDAR Imagery, Seattle, Washington. U.S.

Schulz (2004) described the creation of a GIS landslides map of the Seattle region based on LiDAR data. An extensive record of historic landslides in the Seattle region had already been created prior to this study. However, this historic landslide database was limited in that it underreported landslides in undeveloped and unpopulated areas, and only included data on modern landslides. Using LiDAR data, landslides were identified solely based on ground surface morphology. The LiDAR model was evaluated

visually to identify potential landslide areas. Sites of potential landslide activity were verified via field reconnaissance which resulted in some changes to the potential landslide areas determined by the LiDAR analysis. Based on the results of the field reconnaissance it was determined that landslides could be consistently identified using the LiDAR data provided the landslide was at least 30m long and several meters high.

Schulz, W. H., (2004). Landslide Susceptibility Estimated from Mapping Using Light Detection and Ranging (LiDAR) Imagery and Historical Landslide Records, Seattle, Washington.

In this report Schulz described an ongoing landslide hazard mapping project in the City of Seattle. A previously produced landslide LiDAR map of the Seattle area was successfully used for identifying approximately four times as many landslides as were previously identified in Seattle's historic landslide inventory. Three types of landforms were identified by the author and mapped based on the LiDAR data, landslides (defined as the debris associated with landslides/slope failures), landslide head scarps, and denuded slopes. The total land area of each landform was mapped, and the density of landslides within each landform type. The author assumed that future landslides would have similar rates of occurrence, therefore giving some ability to predict the areas most susceptible to future landslides. According to the author, this mapping criteria provided advantages over traditional landslide maps and inventories. Traditional zoning in Seattle classified areas as either susceptible to landslides, or not. Using the methodology described by Schulz, it is possible to approximate how much more susceptible one given area is compared to another.

Fall, M., Azzam, R., Noubactep, C., (2005). A Multi-Method Approach to Study the Stability of Natural Slopes and Landslide Susceptibility Mapping.

According to the authors of this paper, an area's landslide hazard is a combination of two factors: (1) quasi-static variables such as geometry, geology and engineering properties which make an area susceptible to landslides, and (2) dynamic factors which trigger landslides. The paper describes three methods currently used for evaluating geologic hazards: expert evaluation, statistical methods and mechanical approach. In order to produce a cost-effective and comprehensive hazard map, a combination of these methods is proposed by the authors.

Chleborad, A.F., Baum, R.L., and Godt, J.W. (2006). Rainfall Thresholds for Forecasting Landslides in the Seattle, Washington, Area.

Chleborad et al. (2006) describes empirical landslide thresholds for the Seattle, WA area developed previously by the same authors (Chleborad, 2000, 2003; Godt, 2004; Godt et al., 2006) and tests/analyzes the exceedances and quantifies the probability of landslide occurrence for exceedances. The cumulative rainfall threshold is defined by rainfall amounts during the last 3 days and the previous 15 days. The rainfall intensity-duration (ID) threshold is defined by the rainfall intensity and the rainfall duration.

Godt, J.W., Baum, R.L., and Chleborad, A.F (2006). Rainfall characteristics for shallow landsliding in Seattle, Washington.

Godt et al. (2006) developed a hypothetical landslide warning system by combining a simple water balance and a rainfall intensity-duration threshold to estimate the antecedent moisture conditions of hillslope materials. Based on the results of their approach, they concluded that rainfall activity alone is not

a particularly reliable method for predicting the occurrence of single landslides. However, the authors stated that the methods described in their paper were slightly more effective at predicting when multiple landslides would occur either on the same day, or within a close period of time.

Guzzetti, F., Reichenbach, P., Ardizzone, F., Cardinali, M and Galli, M (2006). Estimating the quality of landslide susceptibility models.

Guzzetti et al. (2006) used a discriminant analysis to determine landslide susceptibility. The dependent variable for their study is the presence or absence of shallow landslides. The independent variables were quite comprehensive (46 total) including morphological, hydrological, lithological, structural, and land-use information. They also presented an evaluation procedure to quantitatively assess the quality of statistical-based susceptibility models.

Harp, E.L., Michael, J.A., Taprade, W.T., (2006). Shallow-Landslide Hazard Map of Seattle, Washington.

This report describes an ongoing landslide hazard mapping project for the City of Seattle. As described in the report, the City of Seattle has prepared a landslide hazard map based on existing recorded landslides, as well as a map of various geologic units, associated shear strength values for this geologic units and a digital elevation model (generated via LiDAR). Since this hazard map focused on shallow landslides, only detailed information about the surface geologic units is required. Commonly used methods for calculating the factor of safety against infinite slope failure includes SINMAP and SHALSTAB, although these methods do require some knowledge of soil parameters and rainfall. The Seattle hazard map used a simplified method suggested by Jibson (2000) because of variations in material properties and rainfall intensity/duration. This method still requires shear strength data for all soil types included in the GIS model. Further analysis of the data set suggested that a landslide model that only uses slope angle (and does not include any shear strength or rainfall data when attempting to predict landslide susceptible areas) will typically predict the same number of landslides as a model that includes shear strength/rainfall data, but a model incorporating strength data will do a better job predicting landslide location.

Guzzett, F., Peruccacci, S., Rossi, M., and Stark, C.P. (2008). The rainfall intensity-duration control of shallow landslide and debris flows: an update.

Guzzetti et al. (2008) compiled a global database of 2,626 rainfall events that triggered landslides and debris flows. They then developed global intensity-duration thresholds that can be used where local and regional thresholds are not available. To account for climatic differences across the events, the rainfall intensity was normalized by the mean annual precipitation and the rainy-day normal.

Aydilek, A.H. and Ramanathan, R.S. (2013). Slope Failure Investigation Management System. Maryland Department of Transportation State Highway Administration Research Report.

Aydilek, and Ramanathan (2013) developed a soil management system (SMS) for the State of Maryland using a GIS database and map overlays. The data maps were used to identify potentially unstable highway slopes using spatial and statistical analysis.

This study used a semi-quantitative index overlay method for assessing slope stability. Qualitative index overlay was used to characterize spatial and temporal conditions in past instability events to identify slopes with similar conditions that are vulnerable to failure.

Pennington, C., Dijkstra, T., Lark, M., Dashwood, C., Harrison, A., and Freeborough, K. (2014). Antecedent Precipitation as a Potential Proxy for Landslide Incidence in South West United Kingdom.

Pennington et al. (2014) discussed the development of an empirical relationship between landslide occurrence and antecedent precipitation in southwest England and south Wales. The period of the study was between January 2006 and July 2013.

Ramanathan R, Aydilek, A.H., and Tanyu, B.F., (2015). Development of a GIS Based Failure Investigation System for Highway Soil Slopes

Ramanathan et al. (2015) described a GIS-based predicted landslide model developed by the Maryland Department of Transportation. The GIS model accounted for slope height, slope angle, rainfall duration and intensity, vegetation and previous landslides. Each category was assigned a score, and the total score was summed in order to determine the total landslide hazard. Using this score, it made it possible for the authors to determine areas that are susceptible to landslide, even if no historical landslide has been recorded.

Jennings, C.E., Presnail, M., Kurak, E., Meier, R., Schmidt, C., Palazzolo, J., Jiwani, S., Waage, E., and Feinberg, J.M. (2016). Historical Landslide Inventory for the Twin Cities Metropolitan Area.

In an attempt to begin to understand landslide susceptibility in the Twin Cities Metropolitan Area, Jennings et al. (2016) have summarized the effort made to create an inventory of historical failures. Online sources and newspaper archives were scoured for occurrences of landslides and slope failures. Precipitation data was obtained from climate archives and it was found that nearly all of the slides in the inventory occurred between May and October with peaks in June and August.

Samia, J., Temme, A.J.A.M, Bregt, A., Wallinga, J., Guzzetti, F., Ardizzone, F. and Rossi, M. (2016). Do landslides follow landslides? Insights in path dependency from a multi-temporal landslide inventory.

Samia et al. (2016) used a multi-temporal landslide inventory from the Collazzone area in Umbria, Italy to quantify the preferential occurrence of landslides in locations where landslides previously occurred. They also studied the time scales of these legacy occurrences and how they are spatially associated over time. They found that landslides follow landslides and that they happen more frequently within 10 years of previous failure.

References

Aydilek, A.H. and Ramanathan, R.S. 2013. *Slope Failure Investigation Management System*. Maryland Department of Transportation State Highway Administration Research Report.

Carrara, A., Guzzetti, F., Cardinali, M., Reichenbach, P. 1999. Use of GIS Technology in the Prediction and Monitoring of Landslide Hazard. *Natural Hazards.* 20, 117-135.

Chau, K.T. Sze, Y.L., Fung, M.K., Wong, W.Y., Wong, E.L., Chan, L.C.P. 2003. Landslide Hazard Analysis for Hong King Using Landslide Inventory and GIS. *Computers and Geosceinces.* 30, 429-443.

Chleborad, A.F., Baum, R.L., and Godt, J.W. 2006. *Rainfall Thresholds for Forecasting Landslides in the Seattle, Washington, Area - Exceedance and Probability*. U.S. Geological Survey Open-File Report 2006-1064, 35 p.

Cho, S.E., and Lee, S.R. 2002. Evaluation of Surficial Stability for Homogeneous Slopes Considering Rainfall Characteristics. *Journal of Geotechnical and Geonvironemtnal Engineering*. 756-763.

Duncan, J. M., and Wright, S. G. 2005. *Soil Strength and slope Stability*. John Wiley and Sons.

Fall, M., Azzam, R., Noubactep, C. 2005. A Multi-Method Approach to Study the Stability of Natural Slopes and Landslide Susceptibility Mapping. *Engineering Geology*. 82, 241-263.

Godt, J.W., Baum, R.L., and Chleborad, A.F. 2006. Rainfall characteristics for shallow landsliding in Seattle, Washington, USA. *Earth Surface Processes and Landforms.* 31, 97-110.

Guzzetti, F., Carrara, A., Cardinali, M., and Reichenbach, P. 1999. Landslide hazard evaluation: a review of current techniques and their application in a multi-scale study, Central Italy. *Geomorphology.* 31, 181-216.

Guzzetti, F., Reichenbach, P., Ardizzone, F., Cardinali, M and Galli, M. 2006. Estimating the quality of landslide susceptibility models. *Geomorphology*. 81, 166-184.

Guzzett, F., Peruccacci, S., Rossi, M., and Stark, C.P. 2008. The rainfall intensity-duration control of shallow landslide and debris flows: an update. *Landslides*. 5, 3-17.

Harp, E.L., Michael, J.A., Taprade, W.T. 2006. *Shallow-Landslide Hazard Map of Seattle, Washington*. U.S. Geological Survey Open-File Report 2006-1139, 23 p.

Iverson, R. M., (2000). Landslide Triggering by Rainfall Infiltration. *Water Resources Research* (36): 1897-1910.

Jennings, C.E., Presnail, M., Kurak, E., Meier, R., Schmidt, C., Palazzolo, J., Jiwani, S., Waage, E., and Feinberg, J.M. 2016. *Historical Landslide Inventory for the Twin Cities Metropolitan Area*. Minnesota Department of Natural Resources, Division of Ecological and Water Resources.

Jibson, R.W., Harp, E.L., and Michael, J.A. 2000. A method for producing digital probabilistic seismic landslide hazard maps: *Engineering Geology*. 58, 271–289.

Laprade, W.T., Kirkland, T.E., Nashem, W.D., and Robertson, C.A. 2000. Seattle Landslide Study. Shannon and Wilson, Inc. Internal Report.

Montgomery, D.R. and Dietrich, W.E. 1994. A physically based model for the topographic control on shallow landsliding. *Water Resources Research*. 30(4), 1153-1171.

Pennington, C., Dijkstra, T., Lark, M., Dashwood, C., Harrison, A., and Freeborough, K. 2014. Antecedent Precipitation as a Potential Proxy for Landslide Incidence in South West United Kingdom. *Landslide Science for a Safer Geoenvironment*, Vol. 1.

Ramanathan R, Aydilek, A.H., and Tanyu, B.F. 2015. Development of a GIS Based Failure Investigation System for Highway Soil Slopes. *Earth Science*. 9(2), 165-178.

Samia, J., Temme, A.J.A.M, Bregt, A., Wallinga, J., Guzzetti, F., Ardizzone, F. and Rossi, M. 2016. Do landslides follow landslides? Insights in path dependency from a multi-temporal landslide inventory. *Landslides*, DOI 10.1007/s10346-016-0739-x.

Schulz, W. H. 2004. *Landslides Mapped Using LiDAR Imagery*. Seattle, Washington. U.S. Geological Survey Open-File Report 2004-1396, 11 p.

Schulz, W. H. 2004. *Landslide Susceptibility Estimated from Mapping Using Light Detection and Ranging (LiDAR) Imagery and Historical Landslide Records*. Seattle, Washington. U.S. Geological Survey Open-File Report 2004-1405, 16 p.

APPENDIX B1

GEOTECHNICAL REVIEW

resourceful. naturally.
engineering and environmental consultants

BARR

Memorandum

To: Omid Mohseni
From: Brent Theroux
Subject: Review of slope failure report
Date: June 19, 2017
Project: Slope Failure Susceptibility Mapping – Pilot Project for LRRB
c: Brian Albrecht, Aaron Grosser

I have reviewed the report for the Slope Failure Susceptibility Mapping project. Following are my comments, presented in bulleted format.

- I think it would be beneficial to more clearly define the terms "failure" and "susceptibility" for the purposes of the report. Theoretical slope failure is defined by Equation 4-1 in Section 4.2. However, within the context of mapping, my understanding is that **failure** is when a 3-day rainfall event becomes equal to or greater than F (the minimum infiltrating water thickness required to cause failure). **Susceptibility** is therefore the quantitative probability of that 3-day rainfall event occurring.
- If I understand the model and methodology correctly, other than for calibration purposes, past failures do not factor into determining susceptibility. Given the infinite slope theory that underlies the model, I understand this. Yet I think a natural evolution of this project would be to incorporate past failure events into the mapping, or possibly develop a way to factor past events into determining susceptibility.
- Avoid use of the word "predict". As I understand it, the model does not predict failure, it only determines susceptibility of failure. Appears in Sections 4.5 and 8.0.
- (1.2, 5th bullet) – In lieu of "testing" and "tested", I think it's more appropriate to use "calibrating" and "calibrated".
- (1.4) – I think this section is better suited for the Executive Summary. Otherwise it seems redundant to the preceding sections in the Introduction.
- (2.5, Vegetation) – While it's true that trees and woody vegetation can enhance a slope's resistance to failure, they can also be a detriment. In poor-draining soils, root systems can provide extended pathways for seepage. Moreover, once a tree's anchoring root mass becomes disturbed, the sheer mass of a tilting tree can be enough to pull soil out of a slope.
- (2.5, Land Use and Drainage Density) – Drainage areas at or below slopes can also be important. Removal of slope soils due to toe erosion acts to reduce resisting forces and increase the overall slope angle.
- (2.5, last paragraph) – It might be worth clarifying these three factors were selected in order to achieve the objectives for this study (or something along those lines). Land Use/Drainage Density

remains an important factor in landslide occurrences, yet its inclusion posed complications for developing a workable model.

- (3.1) – With a limiting failure depth of 6 feet, how does using the coarser 3-meter resolution LiDAR data affect the final resolution of the mapping?
- (4.2, Figure 4-2) – Suggest adding **A** and **B** to the figure to define plane AB.
- (4.2) – Somewhere in this section, I think it's important to state that the infinite slope theory presented and built into the model assumes *drained conditions* (i.e. no excess pore pressures are present). It's important geotechnically because failures can also occur in *undrained* conditions. Furthermore, be very cautious with incorporating effective cohesion in the model. I don't think there is universal conjecture in the geotech community regarding what typical values of effective cohesion are, the degree to which can be measured, or even whether it actually exists in drained conditions.
- (4.2, 2nd paragraph after Equation 4-1) – "That is, if the numerator of Equation 4-1 is ***less*** than its denominator,…"
- (4.4) – What is the NRCS data based on? Some of the given friction angles may be high for loose or medium dense soils.
- (4.4, 2nd paragraph, 3rd sentence) – "For clayey, ***cohesive*** soils…"
- (4.4, 2nd paragraph, 4th sentence) – "…deeper soil layers are not considered." I don't think this statement is needed since the limiting depth was already established at 6 feet earlier in the report.
- (4.4, 3rd paragraph) – I believe you are conflating effective cohesion with *apparent* cohesion. Effective cohesion is a constitutive soil property that is theoretically always present under drained conditions (but, again, there is on-going debate on this). Root systems are typically considered as contributing to apparent cohesion, which is a transient and non-permanent soil property. True apparent cohesion results from surface tension at the air-water interface that acts to pull adjacent soil grains together – the effect disappears when the soil becomes either too dry or too wet (see also *sand castles*).
- (4.4, Table 4-1) – Any soil type classified as Gravel, Sand, or non-plastic (ML) Silt are deemed *cohesionless* and therefore no cohesion value should be ascribed to them unless supported by valid laboratory test data. I realize that may pose complications with the model, but that is the standard of practice. My personal feeling is that any unfailed sand/gravel/silt slope that requires introduction of any cohesion value in order to demonstrate its stability is, by definition, susceptible to failure.
- (4.5) – How was it determined that the 3-day rainfall would be the most useful for the model?
- (6.1, 5th and 6th paragraphs) – I'm not clear on what is intended to be conveyed in these paragraphs. I'm thinking they should be reworded because I don't think they're necessarily correct as I read them. I can help come up with revised wording, although I may need some clarification on what you're trying to say here.

APPENDIX B2

GEOTECHNICAL REVIEW

resourceful. naturally.
engineering and environmental consultants

BARR

Technical Memorandum

To: Omid Mohseni, PhD, PE
From: Brian Albrecht, PhD, PE
Subject: Slope-Failure Susceptibility Report Review
Date: 6/9/1017
Project: 23621218.00
c:

This memorandum summarized a review of the Barr Engineering Company report titled "Slope-Failure Susceptibility Mapping" dated February 2017.

The overall methodology used to develop the susceptibility maps is valid. The model incorporates precipitation, soil strength and slope angle which are the three driving factors in most slope failures. Although simplistic, the model makes good use of what is publically available for data on a county wide basis. My comments mainly relate to some of the specific inputs into the model.

1. The use of effective cohesion in what is a drained strength analysis is debatable. Much of the soil mechanics literature would indicate there is no theoretical basis for cohession to exist in a drained strength analysis, yet lab work often indicates some amount of "cohesion" may exist in a drained condition. In general it is considered an unconservative assumption to include this term in drained strength analyses. If it is included, the value should typically small (less than 5 KPA) and should be supported by site specific laboratory testing. Some of the values in Table 4.1 are higher than I have ever seen used in a drained analysis in professional practice (400 to 500 psf for the clays) and would likely draw negative review comments from most agencies (USACE for example) even if your lab work suggested it exists. I would reconsider some of these cohesion values.
2. In Section 4.4 there is statement that "effective cohesion" may differ due to roots ect.. This is not correct. Cohesion is an intrinsic property of the soil and is not impacted by roots. The stabilizing impacts of roots, matric suction ect. could be built into the model but they should not be lumped into a soil parameter like cohesion. I know Barr has been using the phrase "apparent cohesion" in some projects and lumping these other stabilizing factors into the soil strength. There is no theoretical basis for adjusting cohesion to account for non-soil related factors.
3. Some of the field capacity data (Table 4.2) seems counter intuitive. I would not expect a sand to have a higher field capacity than a loamy sand or sandy loam.
4. I understand the reasons why runoff was eliminated from the model. Long term I would like to see if there is a way to build this in. The slopes most susceptible to fail during precipitation events are steep enough to have a high percentage of the precipitation run off. Therefore assuming all the water infiltrates seems overly conservative especially with increasing slope

steepness. Perhaps the model seems to work well even with this assumption because of the unconservative use of cohesion (i.e. compensating errors). It would seem that there may be a way to build in a certain percentage of runoff based on slope angle.

5. The other long term upgrade that might be useful is to find a way to bring in the 1m contour data. This may not need to be part of developing the initial map, but one of the primary ways a geotechnical engineer looks for slope failures in a desktop type of study is to look for discontinuities in slope faces, which were purposely smoothed out with 3m data. If the areas that are identified as problems with the 3m data, could be more closely examined with 1m data, it may be possible to identify historic slide areas on the mapping off the LiDAR data.

APPENDIX B3

GEOTECHNICAL REVIEW

resourceful. naturally.
engineering and environmental consultants

BARR

Technical Memorandum

To: Omid Mohseni, PhD, PE
From: Ivan Contreras, PhD, PE
Subject: Slope-Failure Susceptibility Report Review
Date: June 12, 2017
Project: 23621218.00

This memorandum summarizes my review of the Barr Engineering Company report titled "Slope-Failure Susceptibility Mapping" dated February 2017.

1. The work is a good effort and first approximation to establish a process to assess the likelihood of slope failures induced by rainfall. There are several assumptions that are made during the process which are explained in the report. From the six major factors listed as impacting the slope failures only three are assessed due to the data availability (slope angle, soil type, and rainfall). In that regards, I suggest that the title of the report be modified from Slope Failure Susceptibility Mapping to "Rainfall Induced Slope Failure Susceptibility Mapping." That would be more reflective of the major factor incorporated into the model.
2. In regards to ways to improve, I think that one aspect that could help in further developing is the assessment of the infiltration of the rainfall water into the soil as a function of the soil type based on the unsaturated conductivity. I have some ideas that would like to share that may help in future developments. This ties to the following comment.
3. One aspect that could be very beneficial would be to incorporate the effect of the suction on the whole picture. The loss of matric suction is a fundamental factor that let to rainfall induced slope failures because of the effect of water killing that negative pressure that in many cases are the major contributors to keep the slope standing. In the majority of the cases the upper portions of the slopes are unsaturated and the negative pressure plays a major role in stability. One of the references indicated that (Cho and Lee). I think this is a key for future improvement. In my view the use of cohesion in the formulation is at least questionable.
4. Another aspect that could be beneficial for improvement is the incorporation of the old landslides into the database which can be reactivated by rainfall. GIS along with LIDAR could be used as a tool for identification of those features.
5. In section 4.2 under Mathematical Model, it is stated that the plane of failure is somewhat arc-shape. I suggests that this sentence be re-worded. The failure surface is much more complex that an arc-shape and there are multiple factors affecting it. You can say that the shape of the failure surface is very complex but it is commonly simplified as an arc-shape.
6. In the geotechnical world the friction angle is typically represented by the following symbol: ϕ' rather than the one shown in the document.
7. Section 4.2, page 12. The term specific weight is not commonly used in the geotechnical world. Consider using the name unit weight instead.

8. Similarly, the term SG described as the bulk specific gravity is confusing for the geotechnical engineering. I understand it as the unit weight of the soil divided by the unit weight of water.
9. In section 4.4, second paragraph Terzaghi is reference in a double fashion and is wrongly written as a reference. It should be mentioned once as follows: Terzaghi et al. (1996).
10. In the same paragraph in the last sentence where it says: is still the best way. Suggest to change to: is still a good way.
11. Under table 4-1 the angle theta (angle of the slope) is listed to represent friction angle. Very important to correct because it can cause a lot of confusion.
12. Tables 4-1 and 4-2 can be significantly improve based on some ideas that I can share with you for the next phase.
13. In section 5.2, I suggest to change the word instigate by initiate. First and fifth paragraphs.
14. In section 8, summary and conclusions, I suggest to delete the last paragraph. I suggest that the language form that paragraph be used in the submittal letter rather than the report.
15. Finally, in 1999, there were severe landslides induced by rainfall in Venezuela, just when I started at Barr. Trying to use this model or a modification of it in that case history would be a nice exercise for verification.

APPENDIX C

HYDROLOGIC REFINEMENT

resourceful. naturally.
engineering and environmental consultants

BARR

Technical Memorandum

To: Project Folder
From: Cory Anderson and Omid Mohseni
Subject: Hydrologic Refinement of GIS-based Slope Stability Model
Date: November 15, 2017
Project: 23/62-1218.00 – 002 - 200

Herein we worked on the improvements to the hydrologic part of the model. A new model was developed and was tested in Excel that can provide a significant improvement to reliability of the results of the GIS-based model of slope failure susceptibility.

1.0 Summary of previous GIS-based tool and areas for refinement

The previous work, described fully in Barr's February 2017 report, used the infinite slope stability theory, commonly used in other physically-based approaches. Using Coulomb's law of friction and assuming seepage parallel to the plane of failure, the factor of safety can be determined based on soil properties and the quantity of water in the soil column (Equation C-1). A factor of safety less than one (1) results in slope failure. The equation determining the factor of safety can be re-written to determine the critical depth of water in the soil column to cause a slope failure.

$$FS = \frac{C + [(\gamma_{sat} - \gamma_w)h/\cos^2\theta + \gamma(Z - h/\cos^2\theta)]\cos^2\theta\tan\phi}{[\gamma_{sat}h/\cos^2\theta + \gamma(Z - h/\cos^2\theta)]\sin\theta\cos\theta} \qquad \text{Equation C-1}$$

The parameters in Equation C-1 are the same as in the main report. The few key areas in the previous model that were reviewed are listed below.

1) In the previous model, the critical depth of water was assumed to be a direct reflection of the depth of a rainfall event. Because of the broad application of the GIS-based model, a simplifying assumption was made that all rainfall is infiltrated into the soil to the plane of failure before any surface runoff occurs.
2) Contributing drainage area to a cell was not considered to determine the water conditions in the soil prior to a rainfall event.
3) Water loss from the soil column due to groundwater flow parallel to the failure plane was not included in the GIS-based tool. In essence, the entire rain event infiltrates, and no water flows out of a given cell during the rainfall event.
4) The duration of the critical storm event was assumed to be three days and no other durations were assessed for the potential to cause slope failure.

2.0 Updates to the GIS-Based Model

There are two papers that were primarily used in the update to the GIS-based tool. The first is a paper by Richard Iverson in 2000 in the journal Water Resources Research that incorporated both long-term groundwater flow and short term steady infiltration rates (rather than only infiltration depths) in the determination of soil water pressure and potential for failure (reference (2)). The second paper in the Journal of Geophysical Research in 2005 expanded on the first work to look at the impact of non-uniform or unsteady infiltration rates (reference (3)). The storm non-uniformity was not incorporated into this tool at this time, but has been shown to have an effect, depending on whether the peak intensity of the storm is early, in the middle, or late in the storm.

The updated model is separated into two main parts, and the individual steps of each part of the model are described in the sections below.

2.1 Updated Model – Part I

The main functions of the first part of the GIS-based model are to filter out grid cells that are "unconditionally stable" and to determine the critical soil water pressure in those grid cells that may be susceptible to fail. The process is described below and dimensions listed reference Figure 4-2.

1) The soil depth, *Z*, is assumed to be 6 feet (1.83 meters).
2) The soil and surface properties at each grid cell are determined from available data and from estimations. These are:
    a. The steepest slope of the surface, θ (degrees), is based on 3-meter LiDAR data.
    b. The friction angle of the soil, ϕ (degrees), is based on the USCS soil classification (see Table C-1) or the plasticity index (see Equation 5-1).
    c. The field capacity of the soil is based on the SSURGO dataset.
    d. The bulk density of the soil, γ (kN/m^3), is based on the SSURGO dataset.
    e. The saturated bulk density of the soil, γ_{sat} (kN/m^3), estimated from Equation C-2 by assuming a specific gravity for non-organic soils (2.65) and the field capacity of the soil. This equation is similar to Equation 4-3.

$$\gamma_{sat} = \gamma_w(1 - FC) + \gamma\left(1 - \frac{1}{2.65}\right) \qquad \text{Equation C-2}$$

    f. The cohesion of the soil (*C* [kPa]) based on the USCS soil classification (see Table C-1).
    g. The saturated hydraulic conductivity of the soil (K_{sat} [m/day]) based on the SSURGO dataset.

h. The slope of the volumetric water content versus pressure head curve near saturation (C_o [1/m]) assigned per soil type based on typical van Genuchten parameters for different soil types (see Table C-1).

Table C-1 Relationship between Soil Type and Cohesion, Internal Angle of Friction, and Slope (C_o) of the Volumetric Water Content versus Pressure Head

USCS Soil Class	Description	Cohesion, C (kPa)	Friction angle, φ (°)	C_o (1/m)
CH	clay of high plasticity, fat clay	25	eq	0.01
CL	clay of low plasticity, lean clay	20	eq	0.01
CL-ML	silty Clay	10	eq	0.01
GC	clayey gravel	0	eq	0.001
GC-CL	clayey gravel with many fines	3	eq	0.001
GC-GM	clayey, silty gravel	5	eq	0.001
GM	silty gravel	0	36	0.001
GM-GL	silty gravel	0	35	0.001
GP	poorly graded gravel	0	38	0.001
GP-GC	clayey, poorly graded gravel	1	eq	0.001
GP-GM	silty, poorly graded gravel	0	35	0.001
GW	well-graded gravel, fine to coarse gravel	0	40	0.001
GW-GM	silty, well-graded gravel	0	35	0.001
MH	silt of high plasticity, elastic silt	5	24	0.01
MH-O	elastic silt w/ organics	0	24	0.005
ML	silt	0	33	0.04
ML-O	silt w/ organics	0	33	0.04
OH	organic clay, organic silt	10	22	0.01
OL	organic silt, organic clay	10	25	0.01
PT	peat	0	10	0.001
SC	clayey sand	0	eq	0.06
SC-CL	clayey sand with many fines	5	eq	0.12
SC-SM	clayey silty sand	5	eq	0.05
SM	silty sand	0	34	0.05
SM-SL	silty sand with many fines	0	34	0.04
SP	poorly graded sand	0	36	0.001
SP-SC	poorly graded, clayey sand	3	eq	0.001
SP-SM	poorly graded, silty sand	0	35	0.001
SW	well-graded sand, fine to coarse sand	0	38	0.02
SW-SC	well-graded, clayey sand	3	eq	0.02
SW-SM	well-graded, silty sand	3	35	0.02

3) Each grid cell is checked with Equation C-3 to see if the grid cell is "unconditionally stable". This is defined by filling the entire soil column with water to the surface (i.e., $h/\cos^2\theta = Z$) and checking whether the factor of safety (*FS*) is greater than or less than one. If the factor of safety is greater than one, the grid cell is deemed "unconditionally stable", and no further calculations in that grid cell are performed.

$$FS = \frac{C + (\gamma_{sat} - \gamma_w)\, Z \tan\phi}{\gamma_{sat}\, Z \tan\theta} \qquad \text{Equation C-3}$$

4) For those grid cells where there is the potential for failure, the critical soil water pressure (ψ_{crit}) and the dimensionless critical soil water pressure (ψ^*_{crit}) are determined with Equations C-4 and C-5, respectively, assuming slope-parallel subsurface flow. Note that equation C-4 is similar to Equation 4-1, with being ψ_{crit} being the same $H_{cr}\cos^2\theta$.

$$\psi_{crit} = \frac{C + \gamma Z(\cos\theta)^2(\tan\phi - \tan\theta)}{[(\gamma_{sat} - \gamma)(\tan\theta - \tan\phi) + \gamma_w \tan\phi]} \qquad \text{Equation C-4}$$

$$\psi^*_{crit} = \frac{\psi_{crit}}{Z} = \frac{C + \gamma Z(\cos\theta)^2(\tan\phi - \tan\theta)}{Z[(\gamma_{sat} - \gamma)(\tan\theta - \tan\phi) + \gamma_w \tan\phi]} \qquad \text{Equation C-5}$$

5) The dimensionless soil water pressure is separated into two parts: a long-term soil water pressure (ψ^*_0) in Equation C-6, and the short-term response to a precipitation event (ψ^*_1). The dimensionless long-term soil water pressure is primarily driven by the upstream groundwater contributing area, *A* (m^2), which is assumed to be equal to the upstream watershed area of each grid cell, and the long-term infiltration rate upstream of a grid cell, *q* (m/day). The long-term infiltration rate was initially assumed to be 5 inches per year in Carlton County based on net precipitation minus evapotranspiration, Figure C-1 (reference (3)). The term ψ^*_0 is defined as $W\cos^2\theta$, where *W* is called the long-term wetness or the ratio between *h* and *H*.
6) Equation C-7 is used to determine the critical dimensionless soil water pressure due to a precipitation event that would cause a slope failure ($\psi^*_{1,crit}$). This parameter is used in the second part of the model.

$$\psi^*_0 = \frac{qA}{bK_{sat}H\sin\theta} = \frac{qA}{bK_{sat}Z\tan\theta} = W(\cos\theta)^2 \qquad \text{Equation C-6}$$

$$\psi^*_{1,crit} = \frac{C + \gamma Z(\cos\theta)^2(\tan\phi - \tan\theta)}{Z[(\gamma_{sat} - \gamma)(\tan\theta - \tan\phi) + \gamma_w \tan\phi]} - W(\cos\theta)^2 \qquad \text{Equation C-7}$$

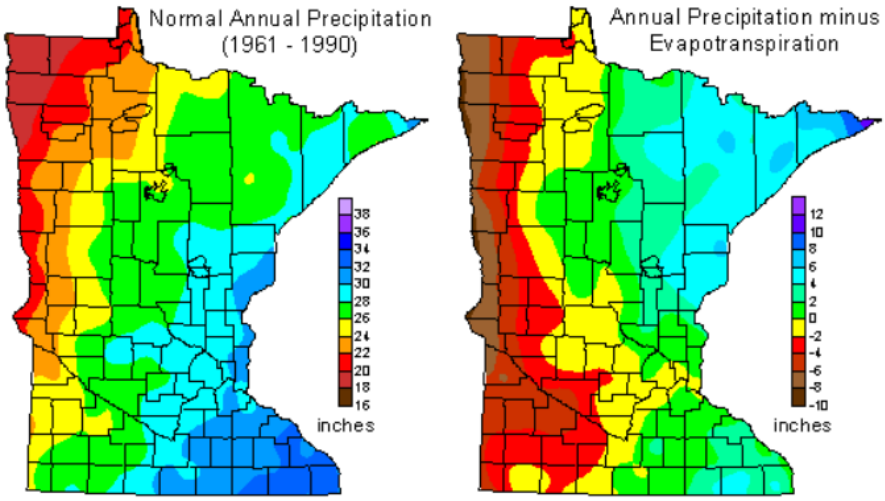

Figure C-1 State-wide normal annual precipitation and net precipitation (*q*)

2.2 Updated Model – Part 2

The second part of the model calculates the dimensionless peak transient soil water pressure ($\psi^*_{1,p}$) due to a precipitation event for a variety of storm durations and annual exceedance probabilities (AEP), i.e., return periods. The values can be directly compared to the critical dimensionless soil water pressure ($\psi^*_{1,crit}$) due to a precipitation event to determine if the slope is susceptible to failure or not for the suite of storm durations and the AEPs assessed.

The derivation of the following approach is shown in great detail in Iverson's paper (reference (1)) and in lesser detail in the follow-up paper (reference (2)). The basic approach assumes the following: Richards equation governs the unsteady, variably saturated Darcian flow of groundwater, relatively wet initial conditions which are commonly prevalent when rainfall triggers landslides, the primacy of pressure-head driven diffusion, and boundary conditions stating that vertical flux is nearly zero at the lower boundary and primarily steady state pressures exist, and at the surface Darcy's law governs infiltration up to the maximum rate of K_{sat}. The solution to the initial boundary value problem posed is shown in Equation C-8 and Equation C-9.

$$\psi^*_{1,p} = \left(\frac{P}{TK_{sat}}\right)\left[R\left(t^*_p\right) - R\left(t^*_p - T^*\right)\right] \qquad \text{Equation C-8}$$

where, $$R(t_p^*) = \left(\sqrt{t_p^*/\pi}\right)\left[e^{\left(-1/t_p^*\right)}\right] - erfc\left(\frac{1}{\sqrt{t_p^*}}\right)$$ Equation C-9

In Equation C-8, *P* is the storm depth in meters, *T* is the storm duration in days, and K_{sat} is the conductivity in meters per day. In Equation C-9, "*erfc*" is the complementary error function.

The process for determining the peak soil water pressure due to the precipitation event is outlined below.

1) First, for each grid cell that has the potential to fail, a diffusivity coefficient, *D* (m^2/day), is determined with Equation C-10.

$$D = 4\frac{K_{sat}}{C_o(\cos\theta)^2}$$ Equation C-10

2) A parameter, T_D (days), is developed using Equation C-11, with units of time to make dimensionless duration and time to peak of soil water pressure. This parameter is unique to each grid cell.

$$T_D = \frac{Z^2}{D}$$ Equation C-11

3) For each AEP tested, i.e., 4% through 0.1% (or return periods of 25 years through 1000 years), and for durations of 5 minutes through 60 days, the storm duration is made dimensionless (T^*) by dividing the duration of storm by the parameter T_D.
4) Based on a soil response curve (see reference (1) and (2)), the dimensionless time at which the soil pressure is maximized (t^*_p) is related to the dimensionless storm duration via the line shown in Figure C-2.
5) For each annual probability, 4% through 0.1% (or return period, 25 year through 1000 year), and for each duration, 5 minute through 60 day, the dimensionless storm duration (T^*) and the dimensionless time to peak soil water pressure (t^*_p) are used in Equation 8 to determine the peak storm-induced transient soil water pressure. The result is a series of curves (Figure C-3) that can be compared to the critical transient soil water pressure ($\psi^*_{1,crit}$).

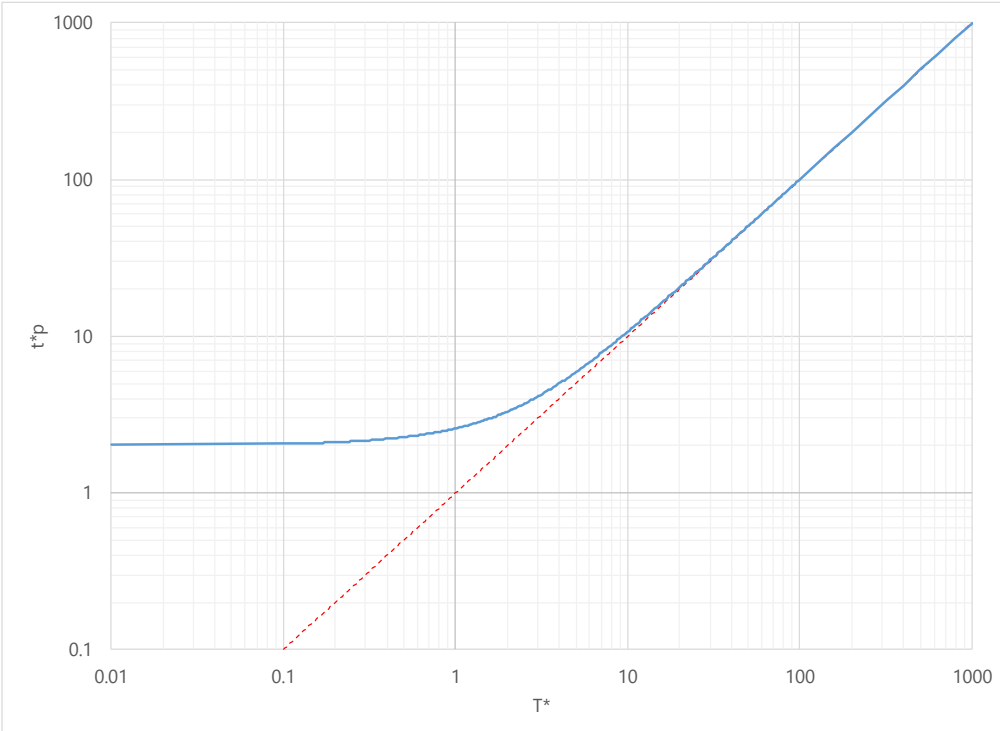

Figure C-2 Dimensionless time to the peak soil water pressure as a function of dimensionless storm duration

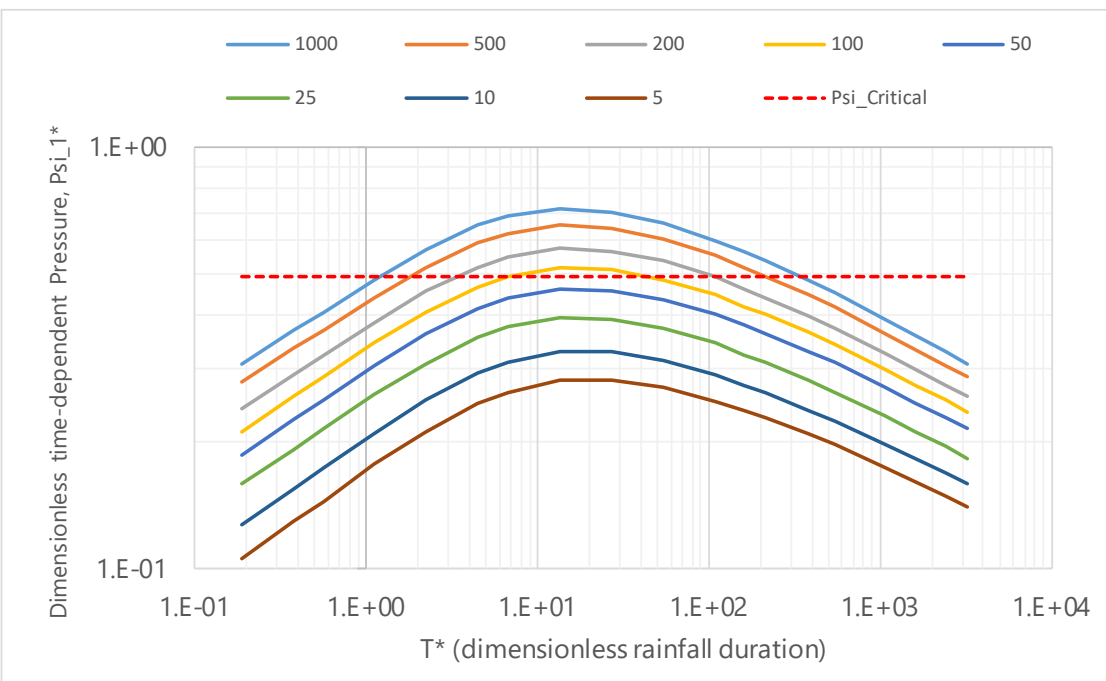

Figure C-3 Example plot of the peak transient soil water pressure due to storm events for a range of return periods (i.e., AEPs) and a range of durations

In the example shown in Figure C-3, precipitation events from the 5-year return period (i.e., with a 20% AEP) to the 1000-year return period (i.e., with a 0.1% AEP) were assessed for durations from 5 minutes through 60 days. The inputs for this grid cell are shown in Table C-2.

Figure C-3 shows that for a given return period, there is a critical duration that produces the highest peak transient soil water pressure ($\psi^*_{1,p}$). Take for example the 100 year storm. For short duration storms (left end of the graph) where the dimensionless duration is approximately 0.19, the storm is short enough and the total precipitation depth is low enough that when the soil column begins to fill with water, the storm stops, and the dimensionless soil water pressure only builds up to about 0.21. Additionally, this soil water pressure is lower than the critical soil water pressure and is not large enough to cause the slope to fail. Therefore, for a storm with an AEP of 0.01 (or a return period of 100 years), with a short duration, the slope is stable.

Similarly, for the long duration storm (right end of the graph) where the dimensionless duration is approximately 3240, the storm is long enough and the uniform intensity is low enough that as the storm starts to fill the soil column with water, the slope-parallel flow out of the cell offsets the infiltration into the cell and the soil water pressure only builds up to about 0.24. Additionally, this soil water pressure is lower than the critical soil water pressure and is not large enough to cause the slope to fail. Therefore, for a storm with an AEP of 0.01 (or a return period of 100 years), with a long duration, the slope is stable.

However, somewhere in between, there is a critical duration where the depth and the intensity are significant enough to cause the highest peak transient soil water pressure. For the 100-year storm, this is approximately where T^* is about 13.5 (or 6 hours, given that TD = 0.0185 for this particular grid cell). For the 6 hour 100-year storm, the peak transient soil water pressure is about 0.52 (about 0.95 meters given Z = 1.83 meters). The assumption that the 3-day storm duration is what controls slope failure has been removed by the refinement to the tool, and in fact, it has been found that in some places, much shorter storms can cause the slope to fail.

Additionally, this soil water pressure is *higher* than the critical soil water pressure and causes the slope to fail. Therefore, for this particular duration 100 year storm, the slope is unstable. Another important note here is that for the 100-year storm, some storms of particular intermediate durations will cause the slope to fail, but not all 100-year storms will. Given the 100-year storm, the range of durations that will cause the slope to fail is a narrow window.

Next, if we take the 1000-year storm event, we see a similar pattern. However, as expected due to larger precipitation depths and intensities relative to the 100-year storm event, the transient soil water pressure is higher. There are still short duration and long duration events that will not cause the slope to fail. However, the range of durations that will cause the slope to fail for the 1000-year storm event is greater, roughly from the 1-hour through the 4-day duration events.

The next thing to observe is that some return periods will not cause the slope to fail, no matter the duration of the storm. For example, for the 5-, 10-, 25-, and 50-year storms, the transient soil water pressure does not build up high enough to be larger than the critical value and therefore does not cause the slope to fail, regardless of the storm duration. For greater events (100-year and larger), there are some storms that will cause the slope to fail, but only a subset of intermediate durations, not all durations. The AEP of slope failure is determined by finding the peak transient soil water pressure curve ($\psi^*_{1,p}$) that is tangent to the critical soil water pressure line ($\psi^*_{1,crit}$). In the case of Figure C-3, the critical storm event is somewhere between the 50-year and 100-year storm event (or between a 1% and 2% AEP). In the tool, the potential for slope failure is classified for each grid cell depending on the highest probability storm event that can cause failure.

If the 3-day storm event was assumed to control for this particular grid cell (shown in Figure C-3), the annual probability of failure estimate could be vastly different. For example, for the 3-day storm event, T^* is approximately 160. Where T^* is 160, the graph shows that the 200-year storm event would not cause the slope to fail, and the 500 year storm would cause the slope to fail. The AEP of slope failure would be between 0.2% and 0.5%, versus 1% and 2%, just for a shorter duration storm.

Table C-2 Inputs for the grid cell with results shown in Figure C-3

Input	Value
Z (m)	1.83
θ (degrees)	41
ϕ (degrees)	33
γ (kN/m^3)	15.0
γ_{sat} (kN/m^3)	19.15
C (kPa)	10
K_{sat} (m/day)	1.0
C_o (1/m)	0.039
D (m^2/day)	181
q (m/day)	0.0002
b (m)	3
A (m^2)	36
T_D (days)	0.0185
100 year, 6 hour storm depth, P (inches)	5.14
50 year, 6 hour storm depth, P (inches)	4.47

References

1. *Landslide triggering by rain infiltration.* **Iverson, R. M.** 7, s.l. : Water Resources Research, 2000, 36(7), 1897-1910.

2. *Potential for landsliding: Dependence on hyetograph characteristics.* **D'Odorico, P., Fagherazzi, S. and Rigon, R.** F01007, s.l. : Journal of Geophysical Research, 2005, 110 F01007, doi:10.1029/2004JF000127.

3. **Minnesota Department of Natural Resources.** Climate's impact on water availability. [Online] [Cited: November 17, 2017.] http://www.dnr.state.mn.us/climate/water_availability.html#space.

APPENDIX D1

CARLTON COUNTY 6-FOOT SLOPE FAILURE ASSESSMENT

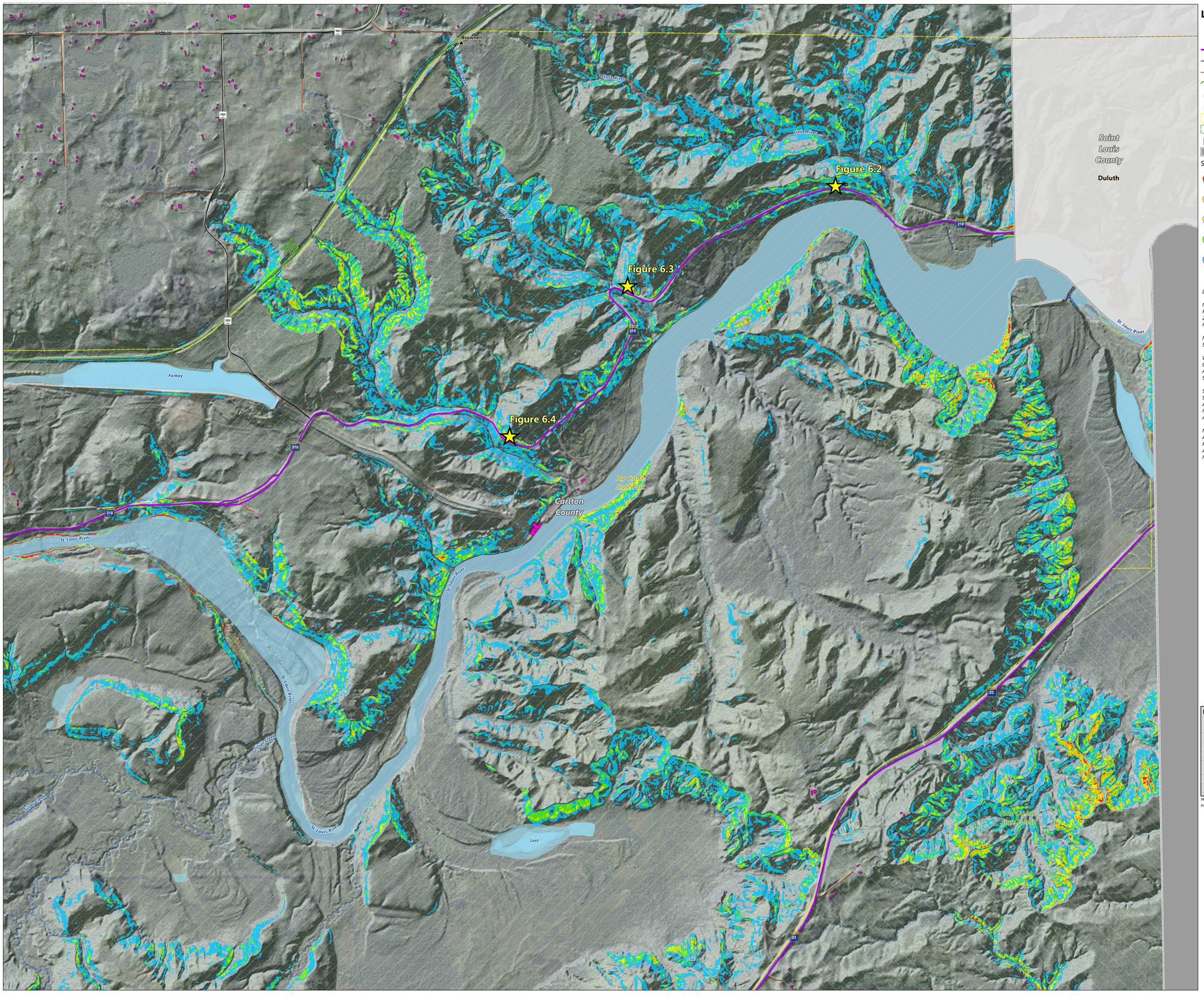

Legend

- Report Inset Map Location
- Populated Place
- State Trunk Highway
- County Road
- Other Road
- State Trail
- Structure Footprint
- Municipal Boundary
- State Park
- State Forest
- County Boundary
- State Boundary

Slope Failure Susceptibility

- Very High (<25-year event)
- High (25- to 50-year event)
- Moderate (50- to 100-year event)
- Low (100- to 200-year event)
- Very Low (200- to 1000-year event)

Data Sources:

National Agriculture Imagery Program (NAIP), USDA FSA. 2015 Aerial Imagery. Available online at: https://gdg.sc.egov.usda.gov

Minnesota DOT. Streets and Highways. Streets_12_14.gdb. 1/12/2014.

Woolpert, Inc. and Minnesota DNR. Carlton County LiDAR Elevation, Arrowhead Region, NE Minnesota. Spring 2011.

Soil Survey Staff, NRCS, USDA. Soil Survey Geographic (SSURGO) Database. Available online at: https://sdmdataaccess.sc.egov.usda.gov. Accessed 9/8/2016.

National Weather Service. NOAA. Atlas-14 Precipitation Frequency Estimates, Partial Duration Series, 3-day. 2013. Availalbe online at: http://www.nws.noaa.gov/oh/hdsc

Feet
500 0 500

Meters
150 0 150

MAP KEY

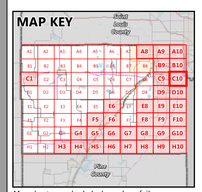

Map sheets are shaded where slope failure susceptibility model results are present

Map C10

SLOPE FAILURE SUSCEPTIBILITY
- 6 FOOT SOILS DATA -
Carlton County, Minnesota

LRRB

BARR

APPENDIX D2

SIBLEY COUNTY 6-FOOT SLOPE FAILURE ASSESSMENT

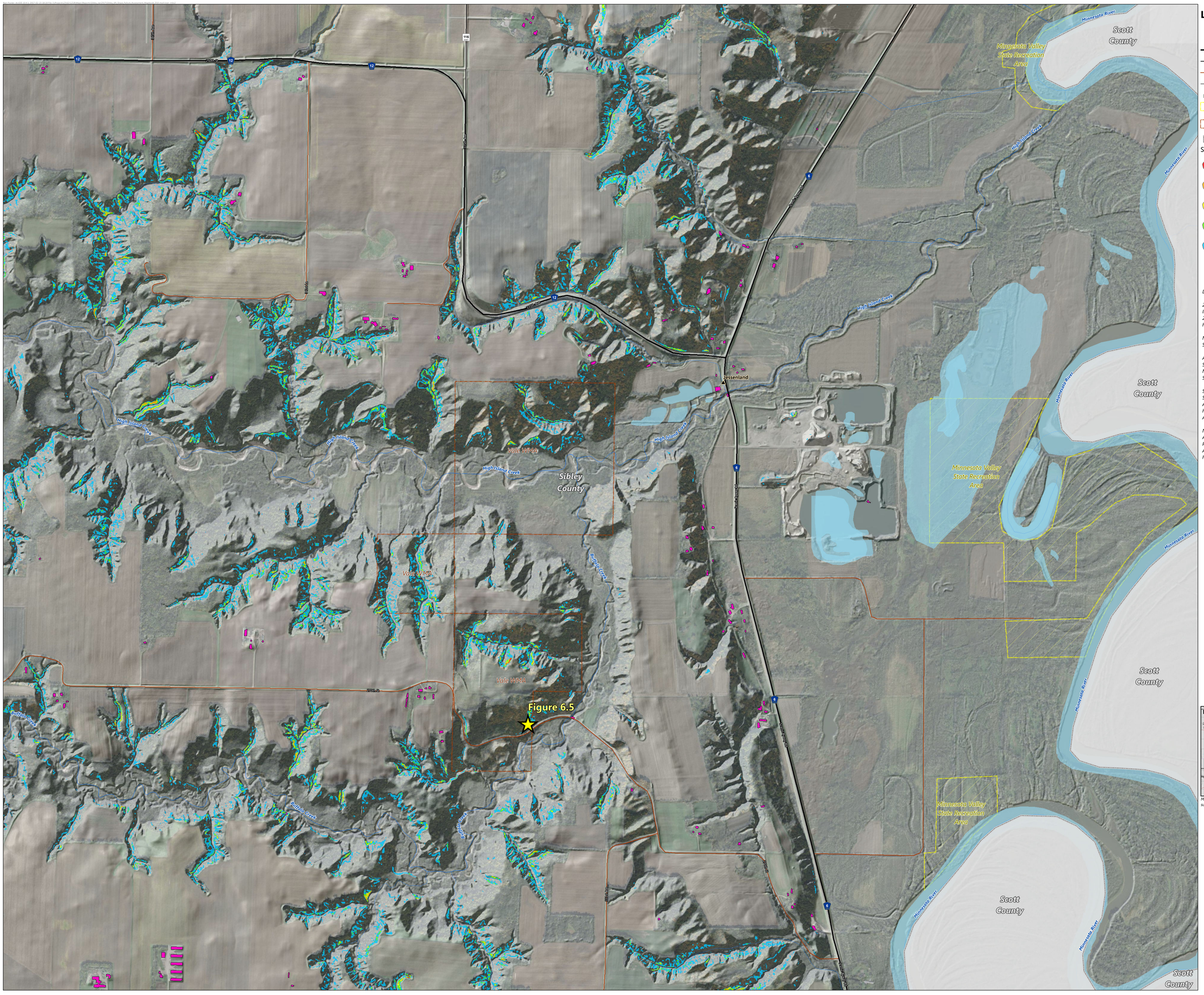

Legend

- Report Inset Map Location
- Populated Place
- County State-Aid Highway
- County Road
- Other Road
- Municipal Street
- Structure Footprint
- State Park
- State Wildlife Management Area
- County Boundary

Slope Failure Susceptibility

- Very High (<25-year event)
- High (25- to 50-year event)
- Moderate (50- to 100-year event)
- Low (100- to 200-year event)
- Very Low (200- to 1000-year event)

Data Sources:

2015 Aerial Imagery. National Agriculture Imagery Program (NAIP). USDA FSA. 2015. Available online at: https://gdg.sc.egov.usda.gov

Minnesota DOT. Streets and Highways. Streets_12_14.gdb. 1/12/2014.

AeroMetric and Minnesota DNR. Sibley County LiDAR Elevation, Minnesota River Basin, Southwest Minnesota, 2010.

Soil Survey Staff, NRCS, USDA. Soil Survey Geographic (SSURGO) Database. Available online at: https://sdmdataaccess.sc.egov.usda.gov. Accessed 9/8/2016.

National Weather Service. NOAA. Atlas-14 Precipitation Frequency Estimates, Partial Duration Series, 3-day. 2013. Availalbe online at: http://www.nws.noaa.gov/oh/hdsc

Feet
500 0 500

Meters
150 0 150

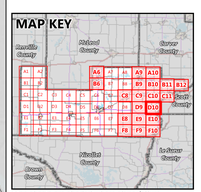

Map sheets are shaded where slope failure susceptibility model results are present

Map D10

SLOPE FAILURE SUSCEPTIBILITY
- 6 FOOT SOILS DATA -
Sibley County, Minnesota

LRRB

BARR